Tissue Engineered Heart Pump Development and Assessment

A Dissertation

Presented to

the Faculty of the Department of Biomedical Engineering

University of Houston

In Partial Fulfillment

of the Requirements for the Degree

Doctor of Philosophy

in Biomedical Engineering

by

Mohamed Ahmed Mohamed Elmahdy

May 2016

Tissue Engineered Heart Pump Development and Assessment

Mohamed Ahmed Mohamed Elmahdy

Approved:

Chair of the Committee
Ravi K. Birla, Associate Professor,
Department of Biomedical Engineering

Committee Members:

Robert J. Schwartz, Cullen Distinguished Professor, Department of Biology and Biochemistry

Elebeoba E. May, Associate Professor,
Department of Biomedical Engineering

Bradley K. McConnell, Associate Professor,
Department of Pharmacology

Ahmet Omurtag, Associate Professor,
Department of Biomedical Engineering

Suresh K. Khator, Associate Dean,
Cullen College of Engineering

Metin Akay, Founding Chair,
Department of Biomedical Engineering

Acknowledgments

To claim success or an accomplishment without acknowledging all those that helped along the way is a crime unlike any other. I certainly would not be where I am today if it were not for the support of my family and friends.

I would like to thank my mother, Fatma Ali, for teaching me that motivation comes from within, and my father, Ahmed Mohamed, for teaching me patience and humility. I would like to thank my older brother and sister, Amrou and Rim Mohamed, who, as a second set of parents for me, have always been role models of perseverance and intellectual pursuit. I would like to thank my little sister, Tasnim Mohamed, who always knew just what to say to cheer me up.

I would like to thank my dearest friends, Omar Khan and Zaki Merliahmad, who have been a great means of escape from the stresses of graduate school and who have kept me connected to the outside world.

I would like to thank my wife, Nesrine Aroua, my greatest blessing. My love for her was forged by the support and wisdom she provided me in my last year of graduate school.

I would like to thank my PI, Dr. Ravi Birla, who has been the most supportive and encouraging advisor any graduate student could have ever asked for. Dr. Birla knew how to perfectly promote creativity and keep us grounded in the lab.

Tissue Engineered Heart Pump Development and Assessment

An Abstract

of a

Dissertation

Presented to

the Faculty of the Department of Biomedical Engineering

University of Houston

In Partial Fulfillment

of the Requirements for the Degree

Doctor of Philosophy

in Biomedical Engineering

by

Mohamed Ahmed Mohamed Elmahdy

May 2016

Abstract

Development of a natural alternative to cardiac assist devices (CADs) will pave the way to a heart failure therapy which overcomes the disadvantages of current mechanical devices. Through implementation of the three principles of tissue engineering, cell sourcing, material scaffolding, and bioreactors, development of a tissue engineered heart pump (TEHP) can be a viable biological CAD option. An experimental model of a TEHP was first fabricated by wrapping artificial heart muscle (AHM), composed of rat neonatal cardiac cells on the surface of a fibrin gel, around an acellular goat carotid artery (GCA) and a chitosan hollow cylinder (CHC) scaffold in various configurations. Histological assessments revealed the presence of cardiac cell layer cohesion and adhesion, as well as retention of cardiac myocyte phenotype. Biopotential measurements revealed the presence of ~2.5 Hz rhythmic propagation of action potential throughout the TEHP. A more clinically applicable TEHP was then fabricated by use of human adipose derived mesenchymal cells (hADMCs), which have been programmed towards a cardiac lineage, in conjunction with a chitosan scaffold imbued with purified porcine extracellular matrix proteins. The second generation TEHP was lined with human endothelial cells and conditioned with pulsatile flow and electrical stimulus. As a result, hADMCs were further matured along their cardiac potential and the TEHPs they embodied formed the foundation for biological CADs.

Table of Contents

List of Figures

Nomenclature

The following acronyms, presented in alphabetical order, are used regularly throughout the text.

3D – Three dimensional

AHM – Artificial Heart Muscle

CAD – Cardiac Assist Device

CHC – Chitosan Hollow Cylinder

DNA – Deoxyribonucleic Acid

ECM – Extracellular Matrix

EMA – ETS2/MESP1 Adipocytes

EMAH – ETS2/MESP1 Adrenergic Stimulated Adipocytes

EMAHR - ETS2/MESP1 Adrenergic Stimulated Rotated Adipocytes

ESC – Embryonic Stem Cell

GCA – Goat Carotid Artery

hADCP – Human Adipose Derived Cardiac Progenitor

hADMSC – Human Adipose Derived Mesenchymal Stem Cell

IABP – Intra-Aortic Balloon Pump

IPSC – Induced Pluripotent Stem Cell

LVAD – Left Ventricular Assist Device

TEHP – Tissue Engineered Heart Pump

1. Introduction

1.1 Tissue Engineering: The New Era of Medicine

Each milestone in the advancement of health is defined by a notable contribution in a particular field. At the turn of the 20th century, the discovery of antimicrobial agents paved the way for the development of antibiotics that revolutionized modern healthcare and dramatically extended our life spans. Nearly 50 years ago, DNA sequencing was performed for the first time, leading the way to paramount discoveries in genetic diseases and drug targets. Humanity now stands at the verge of another major epoch in the advancement of health. At the forefront of this turning point is the field of tissue engineering. The next generation of health will be the direct repair of diseased or damaged tissues and whole organs. Concerns of mortality due to heart attack, kidney failure, liver disease, and so on will be a thing of the past. Simply grow and replace the failed organ. Problem solved.

This feat is no simple challenge, however. Just as the major milestones in the past were met not by a single discovery, but by the contributions of numerous scientific endeavors, the next step will require many such contributions. Tissue engineering is in itself a multidisciplinary field comprising expertise in such areas as cellular biology, material synthesis, and biomedical engineering. These three expertise highlight the main pinnacles of tissue engineering that together lead to the development of biological constructs to replace damaged or diseased tissues and organs. As illustrated in Figure 1, the three areas of focus form the pillars that support tissue engineering. Cell biologists provide the cell source by either isolating primary cells or expanding stem cell lines and possibly tweaking their genetic makeup to encourage attachment, proliferation, and

viability. Material scientists derive suitable materials for these cells with just the right porosity and mechanical characteristics, usually by polymerizing natural and synthetic compounds. Biomedical engineers combine these discoveries and enhance their functionality by the use of customized chambers, called bioreactors, to bring the construct closer to the target organ.

1.2 The Three Pillars of Tissue Engineering

Perhaps the most crucial component of a tissue engineered construct is the cell source. Although a cell cannot recapitulate the appropriate in vivo microenvironment without a support matrix, and a construct will never come close to functioning like its physiological counterpart without a bioreactor, a tissue engineered construct is nothing without cells. The identity of the construct lies within its cellular composition. In fact, most biomaterials are designed to be temporary support structures, which will gradually degrade in vivo and be replaced with a de novo matrix constructed either by the cells that make up the construct or surrounding cells of the host. Extracellular matrix (ECM) is constantly regenerated and remodeled even in adulthood [1]. It is ideal for the cells seeded into the construct to be capable of continuing this natural ECM regeneration, and preferable at a rate faster than biomaterial degradation. For the tissue engineered construct to have any clinical significance, the cell source must not be rejected by the host. One exciting option currently under clinical investigation is the use of reprogrammed host cells. Made using varying protocols, a reprogrammed cell is typically a primary host cell, such as skin or adipose, which is converted into another cell type by downregulation and/or upregulation

of certain cell-type specific genes. By using host cells, the chance for rejection is extremely minimized.

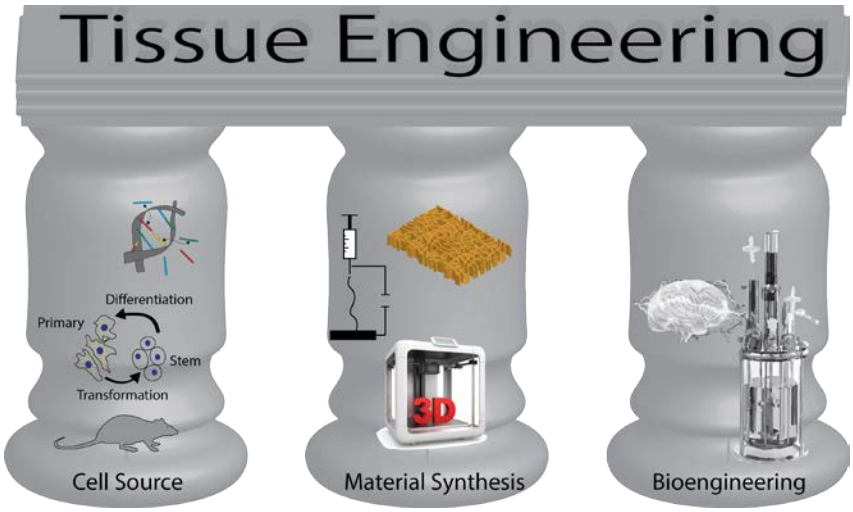

Figure 1. Tissue engineering is a multidisciplinary field supported by three pillars, cell source, material synthesis, and bioengineering.

The biomaterial must also be scrutinized for the risk of host rejection. Biocompatibility of the biomaterial may in fact be the most important asset. A biomaterial can be perfect in mimicking the exact chemical composition, but still have the risk of producing a thrombotic response if the host immune system recognizes any feature as foreign. Acellular biomaterials implanted in the body, such as mechanical heart valves or composite knee implants, obtain biocompatibility by reducing the possibility of cell adhesion. This is not a feasible option however for tissue engineered constructs, which must ensure the adhesion and retention of its cellular components. Biomaterials must also closely match the mechanical characteristics of the target organ, not only to ensure appropriate functionality, such as the case for connective tissue implants, but also to ensure the retention of the appropriate cellular makeup. Cellular differentiation and retention of

cell-type specificity has been shown to be highly influenced to the mechanical characteristics of the surrounding environment.

Bioreactors is the stage of not only functional enhancement, but also validation of the tissue engineered construct. Before clinical implantation, the construct must exhibit cellular viability and functionality close to native organs for an extended period of time. Bioreactors are typically represented as microenvironments for the construct in which it receives a stimulus that will resemble the feedback obtained in vivo. For instance, heart constructs may require electrical or ionotropic stimulus to encourage contraction and improvement of force generation. Kidney constructs may require a perfusion system capable of providing the blood components for filtration and measuring urea output. Bioreactors can also be the technique for cellular aggregation and formation of a self-assembled tissue constructs, such as what is produced in a microgravity bioreactor [2].

1.3 Application of Tissue Engineering

These three pillars of tissue engineering can be applied to any tissue or organ in the human body. The application becomes increasingly more challenging with greater complexity of the organ. For instance, cell sourcing is more complicated if the primary cell of the organ is practically non-regenerative, such as the brain and heart. The belief that both the brain and heart are completely incapable of self-renewal has been debunked by the discovery of stem cell niches within the adult organs [3], [4]. However, the supply of regenerating adult stem cells in these organs is so miniscule that any repair that may take place is negligible. The application is even more challenging for morphologically complex and highly dynamic organs. As such, the heart may well in fact be the most challenging

organ facing tissue engineers. No other organ has as much significance in the optimization of its function. A liver can function at 40% efficiency for the majority of a person's life, but a heart functioning at 40% jeopardizes the functionality of every other organ in the body and dramatically increases the risk of mortality.

The heart is also a primary target for development of tissue engineered constructs due to the overwhelming demand of heart transplantation and repair. Cardiovascular diseases culminate to be the number one cause of mortality in the developed world [5]. By 2030, 43.9% of the US population is projected to have some form of cardiovascular disease. As of now, the only effective long term treatment to heart disease is heart transplant. Effective and long term are both relative terms in that heart transplant has a 5-year survival rate of approximately 75% between 2005 and 2010. In addition, the chance of receiving a heart transplant is nearly 9 in 1000, with roughly 250,000 of the 5.7 million patients with heart failure contending for only about 2,200 donor hearts available each year. Patients on the recipient list are typically provided with a cardiac assist device (CAD) as a bridge treatment.

CADs such as intra-aortic balloon pumps (IABPs) and left ventricular assist devices (LVADs) are examples of commonly used devices to provide circulatory support [6]–[8]. IABPs are anastomosed to the ascending aorta in order to provide after-load reduction, augment coronary artery perfusion, and decrease ventricular workload, thereby improving overall cardiac function [9]. LVADs are used for chronic heart failure and function by pumping blood from the left ventricle to the ascending aorta [6]. The limitations of these devices are associated with thrombogenicity, lack of functional integration at the device-

host interface, the need for long term immune-suppression therapy, and complex control units to regulate device function.

Development of cell-based alternatives will provide novel treatment modalities for heart failure patients, as they will provide the same function of mechanical devices, while alleviating some of their aforementioned problems. Use of autologous cells with biological scaffolding components will eliminate the need for immune-suppression therapy and promote integration at the device-host interface. Biological devices can overcome many of the scientific challenges associated with their mechanical counterparts. Tissue engineered heart pumps (TEHPs) provide a unique alternative to IABPs and LVADs.

1.4 Tissue Engineered Heart Pumps

To tackle the complexity of developing a tissue engineered construct for cardiac regeneration, a simplified heart model construct must first be perfected. This has been conducted by a few researchers in the past under the guise of TEHP development. A TEHP is any tissue engineered construct capable of generating intraluminal pressure to displace a fluid. It is a construct which serves the same function as the heart, without the same physiological complexity. Cardiomyocytes, the contractile cell of the heart, make up the majority of the cellular composition in a TEHP. One of the first attempts to develop a TEHP was performed by Evans and Yost et al beginning in 2003 [10], [11]. By seeding rat embryonic or neonatal cardiomyocytes on collagen-based tubular scaffolds, Evans and Yost were able to measure electrical activity and demonstrate cellular morphology similar to native myocardium. However, neither contractile force nor intraluminal pressure was measured, diminishing their role as TEHPs.

The first reported intraluminal pressure generated from a TEHP came nearly four years later by the work of Kubo et al [12]. By utilizing a self-assembly technique, single-cell layer confluent cardiomyocyte sheets were separated from a temperature responsive surface and sequentially rolled onto a fibrin gel tube. The dimensions of the fibrin gel tube were equivalent to a human carotid artery, at 4 mm outer diameter, 1.5 mm wall thickness, and 40 mm in length. Rolling three sheets onto the fibrin tube resulted in a TEHP capable of generating around 0.1 mmHg of intraluminal pressure. The radial contractile force generated by the TEHP was also measured at maximum pretension to be 185 ± 39 μN. Although a remarkable first step in developing a fully functional 3D cardiac tissue, the generated pressure is nearly 100 times lower than the required median systemic pressure of 100 mmHg. This TEHP was also not capable of spontaneous contraction, and the measured radial forces and intraluminal pressure were a result of electrical stimulation or inotropic response by Ca^{2+} flux.

Over the past decade, ever sense the work of Evans, Yost, and Kubo, TEHP development has been at a standstill. Improvements have been made in cell retention and alignment, expression of key genes for contraction and electrophysiology, and use of clinical relevant differentiable stem cells. However, improvements in the intraluminal pressure generated has not been met. Using the expertise in tissue engineered heart patches developed in the Artificial Heart Lab, development of a TEHP capable of spontaneously generating intraluminal pressures, utilizing a clinically relevant cell source and biomaterial, and multi-stimulus bioreactors, began nearly four years ago. This dissertation provides the steps taken towards the development, as well as insights gained that could be adapted not just for cardiac tissue engineering, but all forms of tissue regeneration and organ synthesis.

2. Cell Sourcing for Tissue Engineered Heart Pumps

2.1 Cardiac Cell Types and Sources

As stated in the introduction, the cell source is perhaps the most important facet of a tissue engineered construct. In fact, most clinical investigation of cardiac regeneration to date utilize either only a cell source or a combination of cell source and liquid matrix. These in-situ cardiomyoplasty techniques, which may involve either direct injection of the cell or cell-matrix mixture to the site of injury or perfusion of the cells in the proximal circulatory system, have so far resulted in limited benefit to patients [13], [14]. All of the clinically tested cells are either embryonic stage, late progenitor stage, or induced pluripotent stem cells. All tests initially aim to renew the cardiomyocyte population within the infarction through trans-differentiation, and the majority of them fall short of this goal [15]. For the most commonly used cell source, bone marrow-derived/circulating progenitor cells, paracrine effects are consistently revealed to be the major mechanism of therapeutic effect [16]. Although a valuable step in discovery of the best cell source for cardiomyocyte generation, current cardiomyoplasty attempts are incomplete trials at whole tissue cardiac regeneration.

The heart is a complex network of diverse cell types, including: cardiomyocytes, cardiac pacing and conduction cells, cardiac fibroblasts, vascular smooth muscle cells, endothelial cells, and cardiac progenitors. Cardiomyocytes are considered the “working” cell type, and their micro contractions culminate in an orchestrated manner to produce the characteristic beating of the heart. Micro contractions are accomplished by the translation of protein structures organized in a striated structure along the axis of the cardiomyocyte, giving them their characteristic appearance. Cardiac pacing and conduction cells are

specialized cardiomyocytes that do not contract, but rather produce and propagate depolarization waves to rhythmically stimulate the working cardiomyocytes. Cardiac fibroblasts, similar to other fibroblasts, maintain the ECM, and are the most proliferative cell in the heart. Vascular smooth muscle and endothelial cells make up the dense vascular network of the heart that deliver more blood by mass than any other organ in the body. Endothelial cells also make up the inner lining of the heart chambers, the endocardium.

The vascular density of the heart is in response to its high energy demand. Cardiomyocytes are enriched with mitochondria to feed the high metabolic activity, which require an immense supply of oxygen and collection of carbon dioxide to prevent hypoxia. Myocardial infarctions are the result of hypoxic incidents that occur due to formation of atherosclerotic plaque that blocks substantial blood supply. The majority of myocardial infarctions occur near the apex of the heart, in the myocardium of the left ventricle, near the bifurcation of the main trunk of the left anterior coronary artery. Zones of myocardial infarction are the target of cardiomyoplasty techniques. However, with the primary interest of renewing the cardiomyocyte population, any regeneration will be at risk of a repeat hypoxic incident if the appropriate vasculature is not present. Therefore, development of a complete cardiac construct that is functional as a standalone tissue, and capable of integrating to the host heart, may become a more effective and prolonged therapy.

The challenge to in-situ cardiomyoplasty, and cell therapy techniques in general, is cell retention at the site of injury. This challenge is all the more prevalent in the heart, due to the dynamic motion and high perfusion rates that hinder cellular adhesion. To make full use of the cell source, a support scaffold should be used during implantation that will be a bridge matrix until de novo ECM can take its place. The support scaffold biomaterial

should be designed around the cell source and mimic the target organ, but the cell source should also cater to the design of the biomaterial. The cell source should be capable of adhering, migrating, proliferating, and surviving in and/or on the biomaterial. Thus, in choosing the cell source, the possible choices for a biomaterial must also be considered.

To validate the idea of developing a TEHP and sustaining cell function in a complex 3D environment, a primary rat neonatal cell source was chosen. Then, to test the feasibility of utilizing a more clinically relevant cell source, human adipose derived cardiac progenitor cells (hADCPs) were used. Both cell types were tested for adhesion and viability on the biomaterials used for TEHP fabrication, which will be discussed in the proceeding chapter.

2.2 Cell Source for Experimental Analysis of TEHP

As a proof of concept for development of a TEHP, primary cardiac cells in the neonatal stage of development were isolated and seeded onto premade biomaterials. These cells are predominantly fully differentiated, but also contain a notable amount of late cardiac progenitor cells. Cardiomyocytes within this cell pool have a greater propensity for survival in culture and are capable of limited proliferation [17]. Although not a clinically viable option, these cells provide a means of assessing the feasibility of developing a TEHP, and the effectiveness of the biomaterial and multi-stimulus bioreactors.

Cardiac cells were isolated from 2-3 day old neonatal Sprague-Dawley rat hearts using an established method [18]. This isolation protocol obtains a mixture of cardiomyocyte, fibroblast, smooth muscle, endothelial, and cardiac stem cells, which are in similar proportion to the natural heart composition. Hearts were cut into fine pieces and suspended in a dissociation solution which consisted of 0.32 mg/ml collagenase type II

(Worthington Biochemical Corporation, Lakewood, NJ) and 0.6 mg/ml pancreatin dissolved in a HEPES buffered saline. Digestion was carried out in an orbital shaker for 5 minutes at 37^{o}C. At the end of the digestion process, the supernatant was collected in 5 ml of horse serum (Invitrogen Corporation, Auckland, New Zealand), centrifuged at 1500 rpm for 5 minutes, and the cell pellet was re-suspended in 5 ml horse serum. Fresh dissociation solution was added to the original, undigested tissue and the digestion process was repeated an additional two to three times. Cells from all the digests were pooled, centrifuged and then suspended in culture medium consisting of M199, 20% F12k, 10% fetal bovine serum, 5% horse serum, 1% antibiotic-antimycotic, 40 ng/ml of hydrocortisone, and 100 ng/ml of insulin.

2.3 Cell Source for Clinical Application of TEHP

The heart contains terminally differentiated cardiomyocytes and too few cardiac progenitors to expand in vitro from a biopsy isolation. A biocompatible and immunologically acceptable cell source must come from elsewhere. The hunt for a clinically viable cell source has yielded a variety of stem cell options, which can be categorized in one of three groups: embryonic stem cells, induced pluripotent stem cells, and autologous multipotent stems cells. Each group has the propensity for cardiac differentiation and has been implemented in a number of clinical trials for cardiac cell therapy techniques.

Embryonic stem cells (ESCs) are the multi-capable cells source used for several cell therapy and tissue engineering applications. Regardless of the stigma behind utilizing ESCs brought about by ethical debates and negative publicity, their pluripotency has

encouraged the feasibility of both in vitro organ growth and in vivo organ regeneration [19]. The usefulness in the pluripotency of ESCs is also its greatest technical challenge. Specific ESC differentiation has low transformation efficiency and preparations are often encumbered with low purity and poor retention of cardiomyocyte progenitors [20]. Genetic instability occurring in vivo runs the risk of detrimental tumorigenic and immunogenic responses.

Induced pluripotent stem cells (IPSCs) were originally generated by the expression of transcription factors in somatic cells, such as fibroblasts [21]. The expression of these key factors, which are detectably upregulated during development and specific to cardiogenesis, is achievable through a reprogramming process using either viral or nonviral vectors, RNAs, or small molecules. IPSCs have a clinical advantage over ESCs, in that they match the host genome, since they were derived from the host, and evade the ethical controversy surrounding ESCs. However, studies have shown that IPSCs may still pose an immunogenic response since the reprogramming procedure may induce both genetic and epigenetics defects [21].

Autologous multipotent stem cells (AMSCs) reside within niches throughout the body well into adulthood, and have the capacity to differentiate into a particular set of lineages. Mesenchymal stem cells (MSCs) for instance, reside primarily in bone marrow and differentiate into skeletal myoblasts, chondrocytes, and adipose tissue [22]. The advantage of AMSCs in general is their narrower lineage specification, which reduces the contamination of non-specific cell types and improves transformation efficiency. AMSCs are also better able to evade immune response since they lack major histocompatibility complexes that may be present in ESCs.

Adipose derived mesenchymal stem cells (ADMSCs) are an immensely more favorable autologous stem cell source than traditional bone-marrow. ADMSCs can be isolated by a less invasive procedure, and have been shown to have a stronger in vitro differentiation proliferation potential [23], [24]. While in vivo differentiation is minimal, early clinical trials for intra-myocardial delivery of ADMSCs have resulted in minor improvement in myocardial perfusion and reduction of induced infarction size by nearly 5% [25], [26]. By guiding the ADMSCs towards a more mature cardiac progenitor, using growth factors, tissue engineered constructs, and bioreactors, a more suitable cell source capable of higher differentiation efficiency may be obtainable.

Through a collaboration with the Center for Molecular Medicine and Experimental Therapeutics at the University of Houston and Texas Heart Institute, a more mature ADMSCs was obtained. Human adipose derived mesenchymal stem cells (hADMSCs) are first infected with a NKX2.5 td-tomato puromycin reporter. hADMSCs are then treated with a TAT-fused proteins ETS2 and MESP1. The TAT-protein delivery system was designed to overcome the leakiness of gene expression along a conflicting differentiation pathway that may occur using conventional lentiviral treatment [27]. ETS2, E26 transformation specific protein 2, is required for the earliest and most fundamental events of murine embryonic anterior-posterior patterning, primitive streak, and mesoderm initiation form the epiblast. MESP1, mesoderm posterior protein 1, preferentially binds to two variants of E-box sequences on DNA and activates critical mesoderm modulators, the embryonic cell portion from which cardiac cells are derived [27].

Treated hADMSCs are forced to aggregate and suspended in a hanging drop, and then plated for activation of the NKX2.5 reporter using Activin A and bone morphogenetic

protein 2 (BMP2). The cells selected using puromycin, which is non-toxic to any cells expressing the NKX2.5 reporter, are considered to be further along the cardiac lineage and become early adipose derived cardiac progenitors (ADCPs). NKX2.5 is one of the earliest markers of cardiac mesoderm, and thus forms a good basis for identifying ADCP [28]. Adrenergic stimulation of the early ADCPs is induced though addition of epinephrine, which encourages the cardiac maturation process by activating the sarcolemma, increasing cell mass and up regulating L-type Ca^{2+} channel currents [29], [30].

ADCPs suspended in epinephrine enriched media are cultured in a slow rotation bioreactor. This exposes the ADCPs to a microgravity environment that keeps them in constant suspension. Microgravity bioreactors have been used extensively to form 3D cell structures through self-assembly or assisted assembly [31]. Cell clusters are then dispersed and suspended in a fibrin gel, and electrically stimulated to induce expression of cardiac specific voltage gated channels and calcium handling proteins. Bioreactos, and their influence on cell culturem will be covered more in depth in the proceeding chapter on bioreactors (Chapter 3). At this point, the ADCPs are on track genetically to become early cardiac progenitors, and will require the use of biomaterial culture and bioreactor conditioning to further their maturity.

3. Biomaterials for Tissue Engineered Heart Pumps

3.1 Biologically Derived and Synthetic Scaffolds

Biomaterials can be described as the restoration or replication of the native environment within an organ. This includes, everything in an organ minus the cells, and is often labeled more specifically as the extracellular matrix (ECM). In the heart, the ECM alone makes up nearly half of the wet-weight. The ECM is gradually produced by its residing cells during development and is constantly undergoing remodeling. The ECM provides the necessary anchorage that enables cellular organization and structural functionality. The challenge with producing the perfect ECM mimic or substitute is where to place the focus. One can either focus on reconstituting the ECM on the microscale, by attempting to reproduce each key component of the ECM, chemically, brick by brick. The other focus is to rebuild the scaffold of the ECM on a macroscale basis, by mimicking mechanical characteristics and structural features.

On the microscale, the ECM accommodates multiple proteins with growth factor and cell receptor binding properties. The complex network obtains functional diversity by glycosylation, the decoration of proteins with added sugars during post-translational modification [32]. The majority of biomaterials currently being researched and validated through clinical trials are limited in this diversification and biochemical functionality. In designing a biomaterial, the mainstream focus is to optimize cell uptake and retention, while minimizing toxicity to residing cells and host tissue. By overlooking the intricate interplay on the molecular level between cell and ECM, a biomaterial should not be expected to stimulate a cellular response to promote endogenous tissue regeneration [33].

In the heart a fibrillary ECM network guides the spatial and temporal synchrony of cardiac development and functionality [33]. If unraveled, the heart reveals a helical-laminar assembly of hierarchically organized fibrillar structures (Figure 2) [34]. Epiphyseal fibers surround the myocardium, perimysial fibers surround groups of cardiomyocytes, and endomysial fibers wrap individual cardiomyocytes (Figure 2) [35]. Within each myofiber, chains of cardiomyocytes are physically connected end-to-end, along their short axes, by intercalated discs containing gap junctions that provide electrical continuity. Myofibers are helically overlapped and arranged into distinct laminas four to six myocytes thick and separated from adjacent laminas by a collagen network. The collagen network provides the backbone of the heart that provides the stiff framework for which the fibrous components of the ECM and the cells depend. The entire helicoid structure is a testament of fiber length economization and ejection fraction optimization. A biomaterial should, thus, mimic the fibrous structure and organization of the native heart in order to optimize function and ensure synchrony between native heart tissue and the construct.

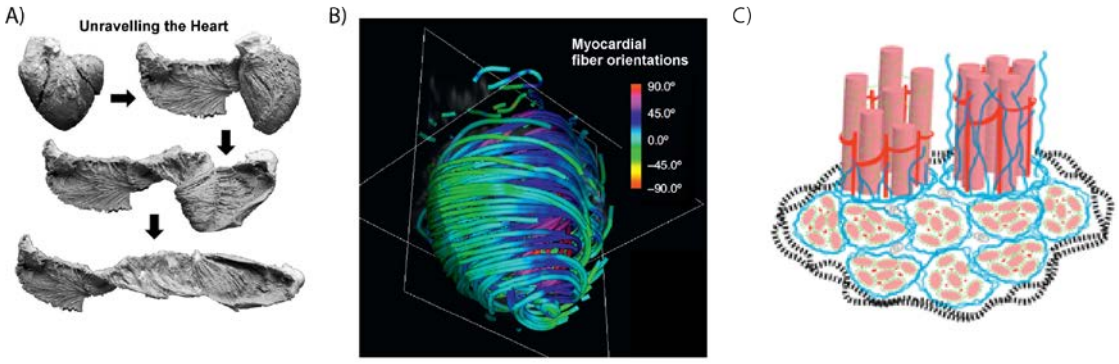

Figure 2. The helical anisotropic fiber alignment of the heart. A) Unravelling the heart through physical dissection shows helical pattern of the muscle fiber. B) Diffusion tensor magnetic imaging color map of myocardial fiber orientation [33]. C) Heart matrix composed of three fiber types [35].

3.2 Artificial Heart Muscle Biomaterial - Fibrin Gel

Fibrin was first purified in large quantities in the 1940s, and has since proven to be a versatile and useful biomaterial for a variety of applications [36]–[39]. Fibrin is naturally formed at the onset of the blood coagulation cascade by thrombin, a serine protease, initiated polymerization of fibrinogen, soluble precursor molecules. Thrombin cleaves the αC domain of fibrinogen to allow for monomer binding as shown in Figure 3. Along with its important role in homeostasis, fibrin is a natural scaffold for tissue repair and remodeling following injury. The fibrin network provides a physical support for fibroblast infiltration, which produce fibronectin, collagen, and other ECM components in their wake to help rebuild damaged tissues. Fibrin also contains numerous binding sites for growth factors and integrins, which provide the necessary signals and cues to direct cell behavior following injury [40]. As a biomaterial, fibrin has been used a cell instructive scaffold for differentiation of stem cells [41], [42], stem cell delivery [43], and induction of angiogenesis [44], [45]. Its popularity as a biomaterial is due to its tunability, ease of use, and compatibility with other polymers to control porosity, fiber thickness, degree of branching, and interfiber distance, which has an effect on the mechanical and functional properties of fibrin.

Due to its versatility, fibrin gel was used for experimental validation of TEHP fabrication and bioreactor activity. As a hydrogel, fibrin gel is an assisted self-assembly scaffold, providing the cells with a simple framework for them to develop their own ECM around. Fibrin is also highly compatible with the experimental cell source, neonatal cardiac cells, due to the inherently high fibrin content in the embryonic and neonatal heart [32]. The combination of fibrin gel and neonatal cells, allow for the recapitulation of early

developmental conditions that allow for cardiac cell adhesion, planar sarcomere organization, angiogenesis, and ECM fabrication (Figure 4). Cardiac cells adhered to the top surface of the fibrin gel and formed a three to six cell thick cardiac muscle layer, depending on the density of cells plated.

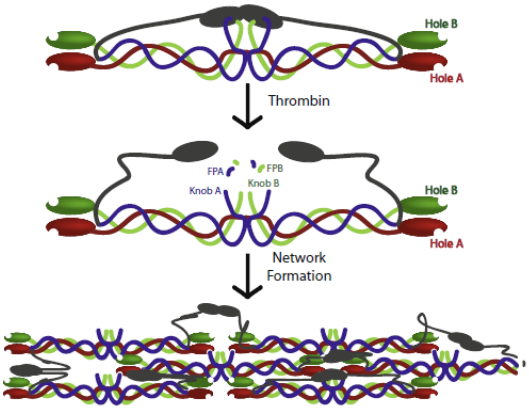

Figure 3. Fibrinogen polymerization by thrombin to form fibrin hydrogels where α chains are shown in blue and β chains are shown in green and γ chains are shown in red. αC domains are shown in gray [40].

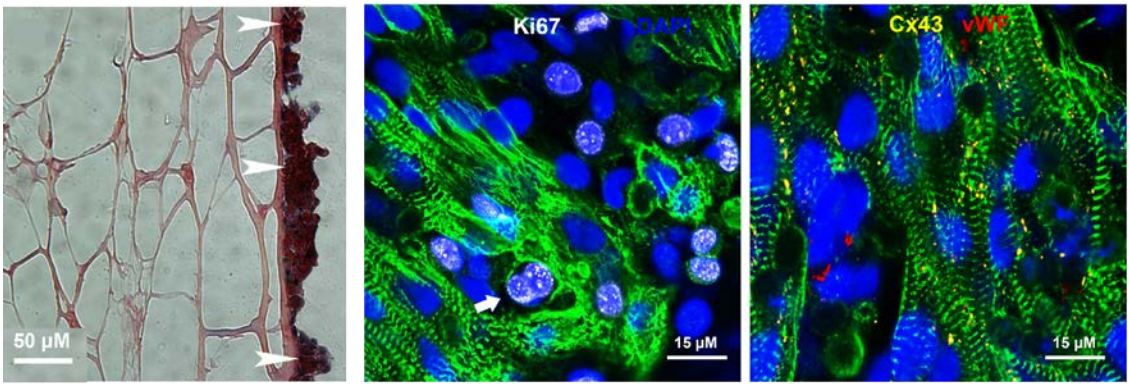

Figure 4. Histology of AHM showing the presence of cardiac myocyte phenotypic expression of sarcomeres stained by α-actinin and gap junction protein connexin 43 (Cx43) at the real cardiac layer on top of the fibrin hydrogel [46].

Cardiomyocytes on the fibrin gel formed bundles with sarcomeres organized perpendicular to the long axis within each cell, similar to native heart morphology. End to end coupling was observed with active gap junction proteins, such as connexin 43, labeled immunohistologically (Figure 4). However, alignment of the cardiomyocytes throughout the entire AHM was not achievable, creating a competitive contraction effort. Despite the lack of cardiomyocyte alignment, the AHM is capable of generating spontaneous twitch forces that rival other tissue engineered cardiac constructs currently under research [47]. AHM twitch forces are cell density dependent, and the optimal density for a two-week culture period was found to be four million cells per milliliter [46]. Twitch forces are also dependent on the pre-tension applied to the AHM during measurement, and the rate of spontaneous contraction. Within a pretention range of 1 to 3 mN, high rate contractions (> 120 bpm) and low rate contractions (< 20 bpm) generated 2602 ± 638 $\mu N/mm^3$ and 3086 ± 804 $\mu N/mm^3$ for AHM plated at a density of four million per milliliter, respectively.

To fabricate an AHM, fibrin gel is first formed by dissolving 5 to 10 mg of fibrinogen in saline. The fibrinogen suspension typically takes an hour to prepare, and requires constant shaking at a temperature of 37°C to improve solubility. A suspension of 5 to 10 units of thrombin per 1 ml of culture media is then prepared. The range of fibrinogen and thrombin concentration used depends on the purity and activity of the components and the desired stiffness of the AHM for its particular application [48], [49]. For instance, AHM used for toxicity or electrical stimulation studies was fabricated with a lower concentration to reduce fibrin gel stiffness and optimize twitch force measurements. Whereas, AHM used for cell transplantation or complex geometry organ fabrication, such as the TEHP, was fabricated with a higher concentration to improve gel rigidity during physical manipulation

and reduce degradation during culture. The ratio between fibrinogen and thrombin is typically 1:1 (mg:units), for all AHM applications.

Throughout culture, fibrinolysis, the enzymatic degradation of fibrin that occurs gradually in vitro as it does in vivo, is inhibited by the use of epsilon-aminocaproic acid (EACA). By inhibiting degradation, the fibrin gel remains intact throughout the entire culture period, and also prevents cellular invagination within the fibrin gel. EACA is a synthetic inhibitor of the plasmin-plasminogen system, and is clinically used intravenously to control bleeding and in hemophiliac compounds [50]. In tissue engineering, the controlled degradation of a scaffold is an extremely powerful tool. Preventing degradation during initial seeding, cellular attachment and alignment, and bioreactor conditioning ensures stability of the construct. After implantation, the gradual degradation of the scaffold allows for the development and full integration of host ECM with the functional cell layers. EACA has been used for exactly this purpose in tissues ranging from artificial heart muscle to cartilage tissues [51]. AHM fabricated for toxicology and bioreactor tests were cultured in EACA supplemented media throughout, while AHM used as a cell transplant method were cultured in EACA free media after transplantation to the secondary support scaffold or geometrically relevant structure.

3.3 Decellularized Native Tissue Scaffolds

One approach to biomaterial synthesis, decellularization, actually requires no synthesis at all. Decellularization is the removal of all cell types from a tissue for use as an acellular transplant or to repopulate with cells for in vitro analysis or regeneration of tissues. Decellularized tissues have been clinically used for heart valve transplants for a

number of years, following the Ross procedure [52]. Along with synthetic mesh options, decellularized skin tissue has been used clinically and offers a more reliable source than autografts [53]. More recently, the first acellular trachea, which was repopulated with host stem cells, was transplanted in 2008 [54]. Ove the past decade, decellularized hearts have also been produced with the prospect of regenerating the whole heart.

The first heart decellularization, repopulation, and heterotopic heart transplantation was performed on a rat by Ott et al in 2008 [55]. The source rat heart was decellularized using the now conventional ionic detergent combination of 1% Triton-X100 and 1% sodium dodecyl sulfate. The now acellular heart was then repopulated with neonatal cardiac cells, which was a combination of cells present in the native neonatal heart obtained in a similar method outlined in Chapter 2. Recellularized hearts after 4 days of culture were able to generate approximately 2.4mmHg, which is 25% of 16-week fetal human heart function and 2% of adult rat heart function. Similar results were achieved by our lab last year in 2015 [2]. More recently, this winter of 2016, the first porcine heterotopic transplantation was performed [56]. Pig hearts were decellularized with the same conventional detergent rinses, but were now seeded with mesenchymal stem cells, a step closer to clinical applicability. The primary goal of the test was to assess the retention of the heart vasculature, coronary blood vessels, perfusivity after implantation. The results suggested that the coronary arteries were occluded almost immediately after implantation and reperfusion. Histology revealed that the artery was filled with thrombi and inflammatory cells throughout the vessel. Considering the findings of immune response from this work and others invalidating its use for clinical application in tissue engineering, decellularized tissues may still provide a useful tool for experimental analysis [57].

As a preliminary step to assess the concept of TEHP development, we utilized decellularized goat carotid arteries (GCAs) in conjunction with the fibrin gel of the AHM. The fibrin gel, in this application, served as the cell transplant vehicle, and the GCA as the complex geometry structural scaffold for fabrication of the TEHP. Vascular anatomy, and in particular that of the major arteries, is quite contrary to that of the heart. Arteries are composed of three distinct, yet conjoined, layers. The intimal layer is the innermost layer composed mostly of endothelial cells and a loose fibrous network of collagen. The medial layer makes up most of the wall thickness of the arteries, and is composed mostly of smooth muscle cells, which is the main differentiator between arteries and veins. The adventitial layer surrounds the artery with a dense collagen network that provides the rigidity that maintains the cylindrical shape and prevents bursting up to 100 times physiological pressures. Between each layer exists an elastic membrane composed of a high concentration of elastin, the protein that provides the elastic properties of the arteries giving them compliance during systolic pressure waves. Arteries are by no means a passive conduit. In response to certain vasodilation and vasoconstriction factors in the blood stream, the smooth muscle cells contract or relax to control blood flow under certain physiological conditions.

Decellularization removes all cell material from the artery, thus, losing this key feature in maintaining homeostasis through hemodynamic response (Figure 5). However, the artery maintains the structural strength and elasticity enabling its use a passive yet still compliant part of the vasculature. Therefore, a decellularized artery provides a suitable framework for physiological conditioning of the AHM to fabricate TEHP. Previous studies have even shown that the mechanical properties of arteries may be conserved after

decellularization [58]. Although the macroscale structure and mechanical properties of the artery remains, decellularization may cause micro fissures in the adventitial and medial layers. These small breaks can damage the vasa vasorum, the microvasculature of the arterial wall. Since the vasa vasorum feeds off of the blood flow passing through the artery, transmural flow can end up leaking into the surrounding medium. This leaking, although minor, is not negligible, and results in gradual declining drifts in transmural pressure and cross contamination of internal and external flows during bioreactor applications.

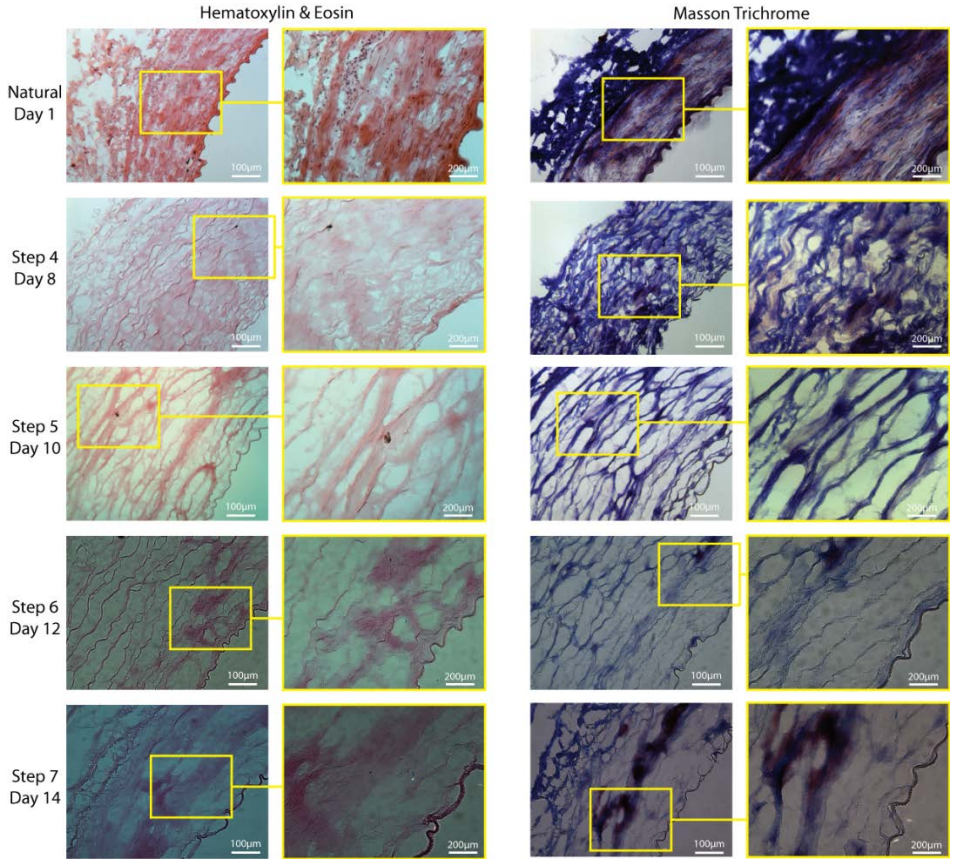

Figure 5. Histology of decellularization progression using a series of detergent washes to remove all cell matter from the goat carotid artery.

3.4 Chitosan Hollow Cylinders

Chitosan is the N-deacetylated form of chitin, the most abundant polysaccharide in natural macromolecules, perhaps second only to cellulose. Chitin is the major component of the shells of crustaceans, including crabs and insects. As such, its source is both abundant and renewable. As a comparison, the price of a common synthetic hydrogel, tetraethylene glycol dimethacrylate (PEG), is more than 10 times the price of chitosan by volume. In its natural state, chitin is hardly biodegradable due to its low water solubility. To facilitate its use as a biomaterial, chitosan oligosaccharides are produced by several methods, including enzymatic and acidic hydrolysis. The chemical representation of chitin, chitosan, and chitosan oligosaccharides is presented in Figure 6. The resulting low molecular weight polymers and monomers are reconstituted through particular freeze and lyophilization (dry freezing) protocols.

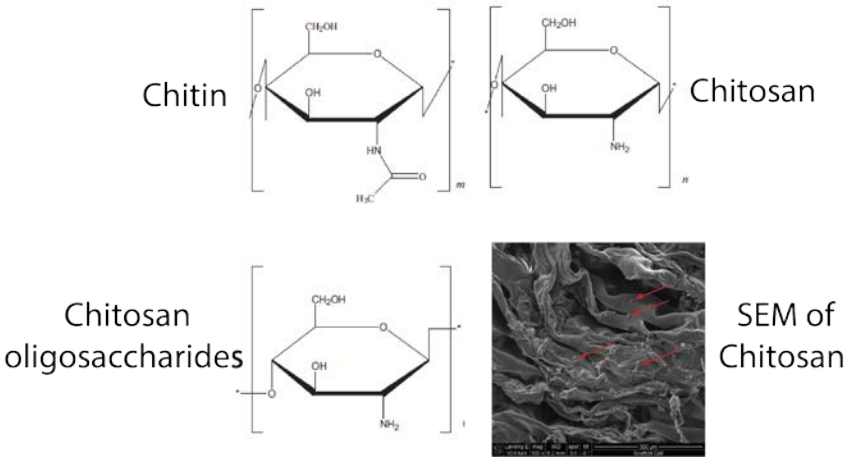

Figure 6. Chemical composition of chitin, chitosan, and chitosan oligosaccharides [59]. SEM image of 2.5% chitosan scaffold.

Chitosan has high mechanical strength compared to other biologically derived hydrogels. In addition, chitosan is biodegradable, biocompatible, non-antigenic, and non-toxic. Chitosan is actually a natural antioxidant, enhancing its role as an anti-inflamatory, antimicrobial, hypocholesterolemic, immunostimulating, and anti-tumor material [59]. To further encourage their use as a biomaterial, chitosan is often used in conjunction with other materials to improve biodegradability and cellular adhesion. Chitosan-collagen hybrid scaffolds, for instance, have shown improved collagen fiber crosslinking alignment and a more reinforced structure for rigid scaffold applications. Considering its superiority compared to other synthesized hydrogel biomaterials, chitosan hollow cylinders (CHCs) were selected to replace decellularized arteries as support scaffolds for TEHP. Since they have less risk of immune rejection and toxicity, as commonly found in decellularized matrices due to remnant detergents and fixatives, CHCs also bring the development of TEHPs closer to in vivo assessments.

Chitosan hollow cylinders (CHC) were synthesized by dissolving 2.5% w/v chitosan (CarboMer Inc., San Diego, CA) in 0.2 M acetic acid solution. The dissolved chitosan mixture is poured into a cylindrical polycarbonate mold measuring 3 cm in length, 3 mm in inner diameter, and 6 mm in outer diameter and frozen at -80°C for 24 hours. The molded chitosan is then lyophilized at 0.1-0.15 mbar of pressure and -40°C for 24 hours (Labconco Freezone, Kansas City, MO). The lyophilized chitosan samples are then rehydrated in 0.1 M NaOH until use. Before use in TEHPs, the CHCs are sterilized in 80% ethanol for 30 min, and washed 3 times in sterile PBS.

Chitosan-ECM hybrid scaffolds, at varying ratios, were also prepared by first purifying ECM. Porcine heart segments were decellularized using the same detergent protocol applied to the carotid arteries for acellular TEHP support scaffold synthesis. The acellular heart segments were then frozen and lyophilized following the same procedure as chitosan synthesis. The lyophilized heart segments were then ground into a coarse powder. The coarse powder was refrozen, re-lyophilized, and reground to obtain a fine ECM powder. The ECM powder was mixed in various proportions to chitosan, and the normal process for chitosan synthesis was followed.

Fourier transform infrared spectroscopy, a chemical characterization technique based on the absorbance of infrared light, performed on chitosan and chitosan-ECM scaffolds showed distinct peaks pertaining to CH_2 and CH_3 bending at ~2800cm^{-1} and to amid I vibrations at ~1700cm^{-1} (Figure 7). These peaks are characteristic of collagen groups and coil structure, as opposed to the chitosan polysaccharide hexagonal ring structure. Imaging of the scaffold ultrastructure was also performed using a scanning electron microscope (SEM). The structure revealed that chitosan-ECM scaffolds contained chitosan sheets laden with ECM granules at ~1μm in diameter. The ECM particles did not drastically interfere with the chitosan sheet formation or crosslinking.

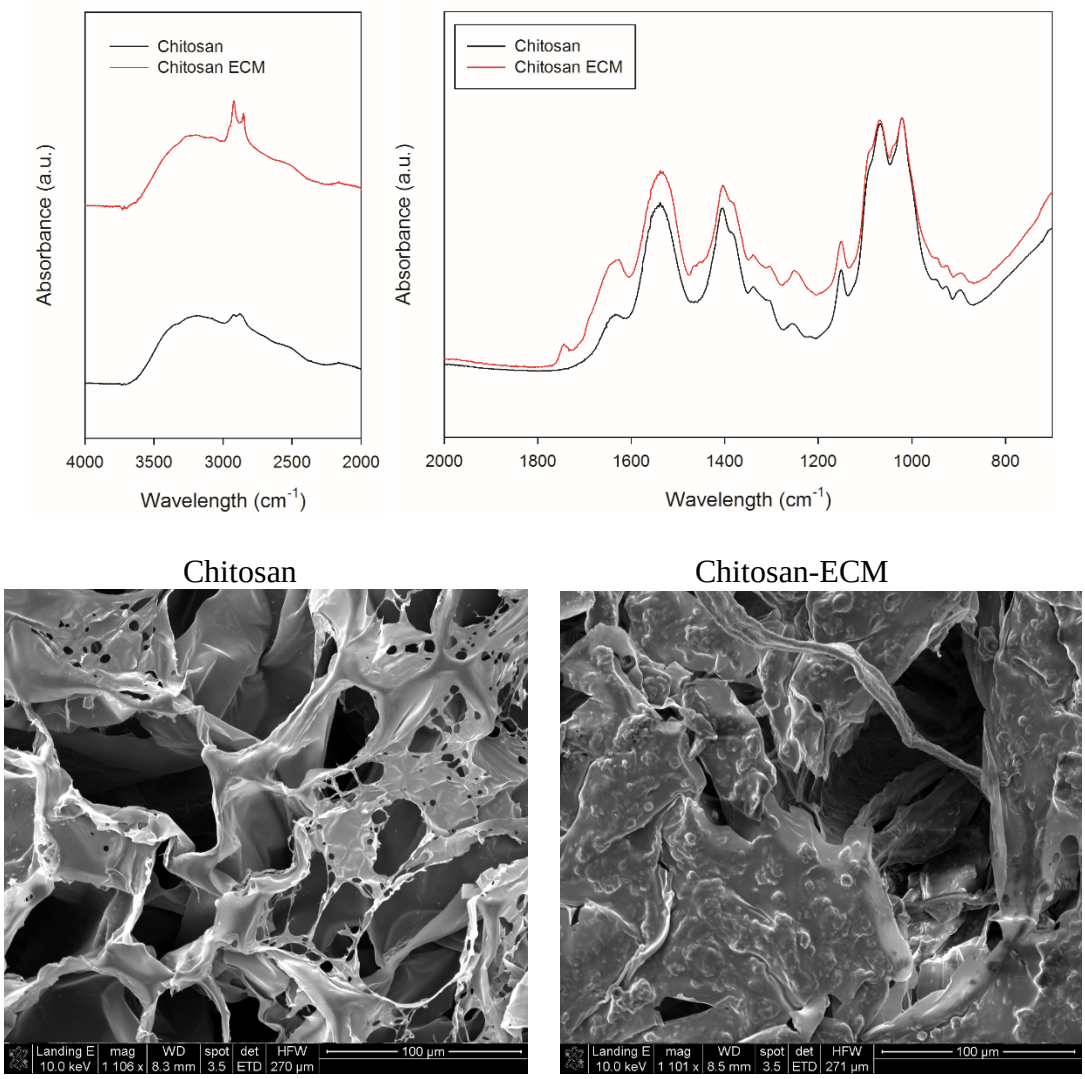

Figure 7. Chitosan and chitosan-ECM spectra and SEM showing presence of collagenprotein chemical components in the spectra and ultrastructure.

4. Bioreactors for Tissue Engineered Heart Pump Development

4.1 Bioreactors for Every Function

Bioreactors have become such an integral part of not only tissue engineering, but in vitro cell culture as a whole. Bioreactors can successfully mimic the in vivo environment, which diminishes cell loss due to apoptosis and phenotypic instability. Bioreactors may also go beyond physiological conditions, and provide optimized environments to enhance certain cellular properties. By definition, a bioreactor is any device or system capable of controlling the extracellular environment by providing certain stimulating ques, nutrient supply, and conditioning to not just sustain cell viability, but surpass the beneficial effects of conventional static culture. For 3D culture, bioreactors are an absolute necessity, since nutrient supply to interior cells beyond a few 100 μm is limited by diffusion alone. Therefore, a perfusion bioreactor, perhaps the most basic form of a bioreactor, is the most essential.

Multistimulus bioreactor systems culminate the enriching effects of a number of stimuli coincidently in one system. Such systems are especially necessary for cardiac tissue engineering, given the dynamic and multi-stimuli physiological environment. Cardiac cells experience mechanical, electrical, and chemical cues at unsteady levels throughout cardiogenesis and adulthood. During cardiogenesis, hemodynamic load is prominent stimulus for proliferation, however, in adulthood, cardiac load may lead to pathological hypertrophy. Hemodynamic load and cardiomyocyte contractility collaborate to influence ECM remodeling as well, which has a recursive effect on heart elasticity and cell phenotype [60]. Electric field potentials influence cell alignment and gap junction protein synthesis during embryogenesis, which optimize conduction of the contraction inducing

depolarization wave throughout and development and adulthood. Endocrine and paracrine stimulation synthetize cardiac myocytes to respond to environmental triggers efficiently.

4.2 Perfusion Bioreactors

Perfusion is an integral part of a bioreactor system considering the high metabolic activity of cardiac myocytes requiring ample supplies of nutrients, efficient respiration, as well as cell waste clearing. In conjunction with the metabolic benefits, perfusion can be a source of vital shear stress for certain cell types. For instance, endothelial cells experiencing fluid shear stress, as the cell-type with direct contact to the fluid environment, better maintain their phenotype and excrete beneficial growth factors for neovascularization and tissue remodeling [61]. Perfusion systems come in all shapes and sizes, and utilize various fluid displacement techniques. The primary objective of perfusion systems is to provide continuous or intermittent flow for cells as opposed to static culture conditions.

The perfusion system fabricated consisted of a custom housing for TEHP, biocompatible silicone tubing interconnected with luer lock and barbed tubing fittings, and a peristaltic pump for fluid displacement. The custom housing allowed for the culture of three TEHP simultaneously, as shown in Figure 8. At short tubing distances, less than 0.5 m away, a peristaltic pump can generate pulsatile flow at pressure ranges from 5 to 20 mmHg, depending on the compliance and diameter of the pump tubing in contact with the rollers of the pump, and the compliance of the interconnected tubing. At long enough distances, however, where the pump is connected to the TEHP housing with more than 1 m of tubing, the pressure generated by the peristaltic pump rollers is minimized. The result

is an almost laminar fluid flow profile at the TEHP. The fluid flow profile was not modeled as Poiseuille flow, since the assumption of no slip and no shear at the inner wall cannot be made in this case.

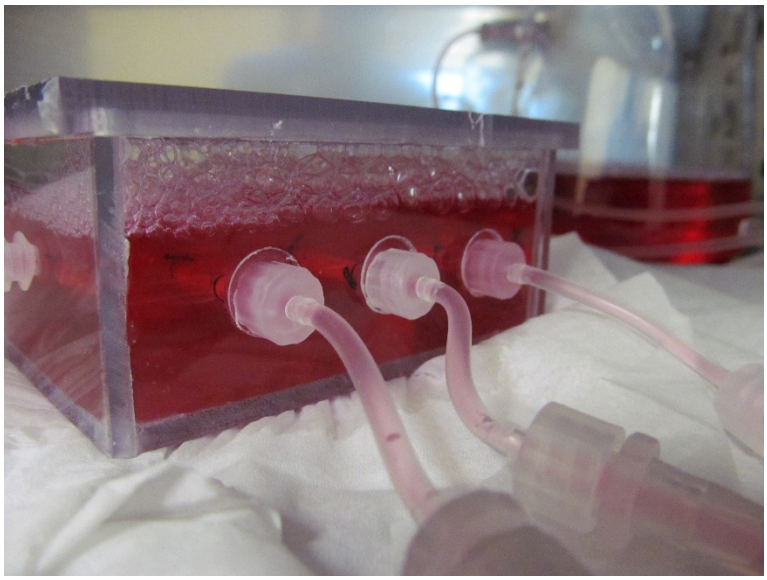

Figure 8. Perfusion bioreactor chamber housing three simultaneously cultured TEHP. Flow is branched from the main fluid line into three intraluminal flows and one immersion bath flow.

Fluid flow was pumped to the TEHP lumen and to an immersion bath simultaneously. A compliance chamber was placed in line to the TEHP chamber and the peristaltic pump to equilibrate the fluid levels between the luminal and immersion flows, and to remove air bubbles that may be generated. The compliance chamber was also used to generate a pulsatile flow, the means of which will be described below in the section on Pulsatile Flow Bioreactor. With the peristaltic pump set to a fluid flow of 80 ml/min, based on the rotational speed of the rollers and the fluid displacement allowed by the 1/4 in inner diameter pump tubing, the fluid velocity at the 3 mm inner diameter TEHP was ~280 cm/min. Based on the assumption of laminar flow in the TEHP lumen, the wall shear stress

would be ~6 dynes/cm^2 or 0.6 Pa, which is the lower limit of arterial wall shear stress in vivo [62].

Within the custom housing, TEHP are connected to luer lock-barbed fittings via 1/8 in inner diameter silicone tubing inserts at each end. The TEHP scaffold is tied and clamped to the silicone tubing by a surgical suture loop and knot. The silicone tubing connects the TEHP to the perfusion system without damaging the TEHP through physical manipulation and minimizes leakage of the luminal flow into the immersion bath. The tubing inserts also help to reduce the effects of recirculation zones appearing at inlet and outlet points, which tend to create areas of stagnation and poor nutrient delivery to TEHP [63]. Nutrient delivery and gas exchange occurs in the capillaries, at which point velocity decreases to ~3 cm/min, due to the pressure drop across the circulatory system and the increased resistance, and not due to reduction in diameter. Since a substantial amount of the nutrient deliver and gas exchange would occur at the external surface of the TEHP, where the real cardiac cell layer resides, the immersion bath, which is a rectangular prism with a 5 by 4cm cross section, was designed so that the fluid flow decreases to ~4 cm/min.

4.3 Pulsatile Flow Bioreactor

Pulsatile flow was the basis of mechanical stimulus to the TEHP. Intraluminal pressures, generated by pressure waves that traverse the fluid flow, induce a radial expansion to the TEHP. The radial expansion induces a strain on the cardiac myocytes, which has been shown to promote cardiomyocyte phenotype retention. The effect on cardiac myocytes is maximized when the long axis of the cell is aligned circumferentially around the TEHP. Mechanical stretch has also been shown to encourage production of

aligned ECM by fibroblasts [64], and optimizes endothelial cell morphology, orientation, and protein expression [65].

Mechanical stretch of the TEHP was induced by the circumferential expansion of the cylindrical construct via transmural pressure variations in the intraluminal flow. One method of applying this pulse is by use of a compliance chamber and an electronic/pressure pneumatic controller. The compliance chamber is the same used as a reservoir for perfusion to maintain equilibrium between the intraluminal flow and immersion bath. Since the compliance chamber is an enclosed chamber with a fluid-air interface, by applying a pressure wave pneumatically, the fluid translates that pressure wave throughout the flow circuit. The pneumatic controller used is a current/pressure (I/P) transducer (T900X, Control Air, Inc.), which is capable of outputting pressures in the range of 0-17psi, or 0-880 mmHg, in a 4-20 mA range. The current for the I/P transducer was controlled using a NI DAQ (PCI 6723, National Instruments), and LABVIEW to generate a current pulse train at the desired frequency and amperage.

The goal of pulsatile flow is to progressively condition the TEHP by mechanical stimulation at four separate stages throughout culture as illustrated in Figure 9. Stage 1 starts at 50 ± 10 mmHg, and each stage increased the baseline by 20 mmHg, until stage 4, which induces pulses at 110 ± mmHg, the physiological pressure range.

4.4 Electrical Stimulation Bioreactor

The cells were stimulated with a biphasic square waveform, illustrated in Figure 10 as measured by an oscilloscope directly attached to the electrodes. In LABVIEW, two monophasic square waveforms of opposite polarity at + or - 2.5V, 3Hz, and 20% duty cycle

were generated with an 80° interphase shift and combined to form the biphasic wave. The stimulus was intermittently delivered to the AHM in one hour segments, with one hour for stimulation and one hour for rest. The pulse amplitude values have been chosen based on previous experimental observations of endogenous physiological currents and dc electric fields [66]. The depolarization wave of a human ventricular cell is approximately 300ms long. During this wave, the intracellular potential is elevated above its negative resting value of -80-90mV to a value nearing 70mV. The anodic wave ensures that the majority of the cells are hyperpolarized and prepared for the depolarizing cathodic wave to induce contractions more synchronously.

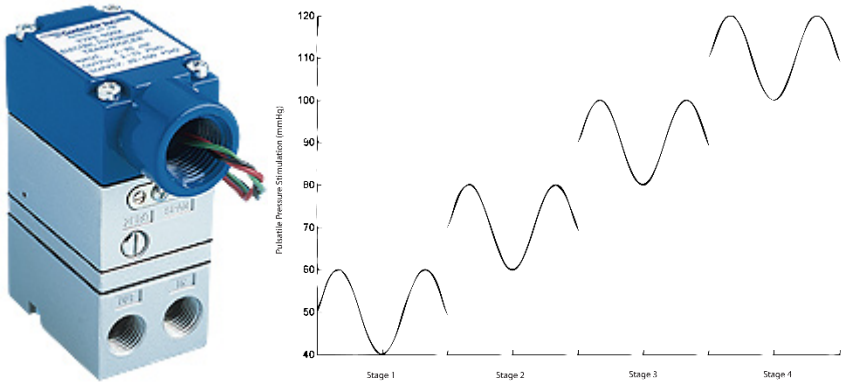

Figure 9. Pulsatile flow generated by a current/pressure transducer (left) to control transmural pressure across TEHP at four distinct pressure wave stages (right).

Relative to monophasic, a biphasic square waveform has been shown to have improved efficacy in ventricular defibrillation clinically [67]. Biphasic electrical stimulation of cardiac progenitor cells has also been shown to more quickly morph them into spindle shaped cells, and to increase expression of cardiac transcription factors,

MEF2D, GATA-4, and NKX2.5, as well as sarcomeric proteins, troponin T, cardiac alpha actinin, and SERCA2a [68]. Use of a biphasic waveform also reduces corrosion of the electrodes and the ensuing release of oxidative species into the culture media [69]. While the stainless steel electrodes used in the electrical stimulation bioreactor are initially biocompatible and nonreactive, extended periods, ~1 month, of use in high electrolyte solutions, such as the culture media, will lead to corrosion. This effect is greatly reduced by use of a biphasic as opposed to a monophasic waveform.

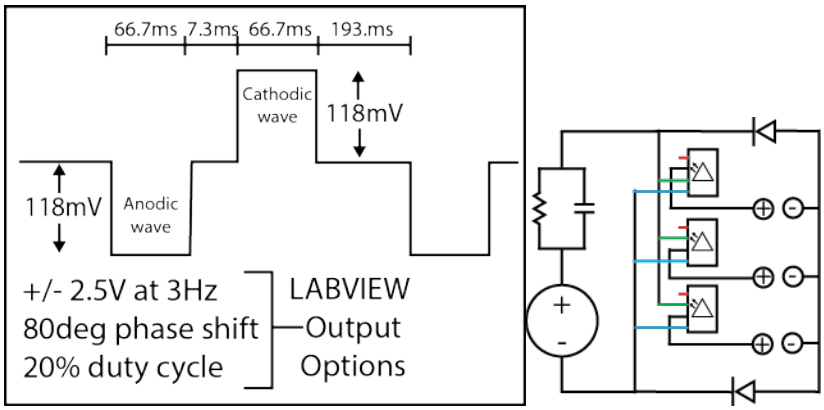

Figure 10. Biphasic pressure waveform output parameters from LABVIEW and measured potentials using an oscilloscope at the electrodes (left) and the wiring schematic for the electric stimulus delivery chamber of the bioreactor (right).

5. Experimental TEHP Results

5.1 Fabrication of Tissue Engineered Heart Pump

A schematic of the TEHP fabrication process is illustrated in Figure 11. The AHM was wrapped around a 3 cm long segment of acellular goat carotid artery (GCA) or chitosan hollow cylinders (CHC) and sealed using silk sutures. The AHM was wrapped around acellular GCA with the cardiac cell-side in either a proximal, between the GCA/CHC and fibrin gel, or distal, exposed directly to surrounding culture media, configuration. A second layer of AHM was also wrapped around acellular GCA in either the proximal or distal cardiac cell layer configuration, to assess the feasibility of multi-cell-layer transplantation. To maintain a cylindrical geometry, a 1/8 inch diameter silicone tube was inserted into the GCA/CHC lumen. The construct was immersed in media within a 15 ml conical tube and cultured for 4 to 12 days with medium changes every two days. The effect of adding aminocaproic acid, a fibrinolysis inhibitor, at a concentration of 2 mg/ml was tested in a parallel gel degradation study.

Synthesis of CHC was consistent and provided a structurally sound tube shape. Histology on CHC did not show contamination of any nucleic material. Porosity of the CHC was nearly 6 times greater than that of natural and acellular GCA, as shown in Figure 12. Localized contraction throughout the TEHP was observable, macroscopically, during the first 2 days after wrapping the AHM. After these 2 culture days, contraction was observed using an inverted microscope with a 4X objective (See supplemental videos). Average thickness of an acellular GCA and a single layer of AHM are 2mm and 700μm, respectively. Once rehydrated, the CHC shrinks to approximately 5.25 mm in outer diameter and 2.5 in inner diameter; thus, a thickness of 2.75 mm is obtained.

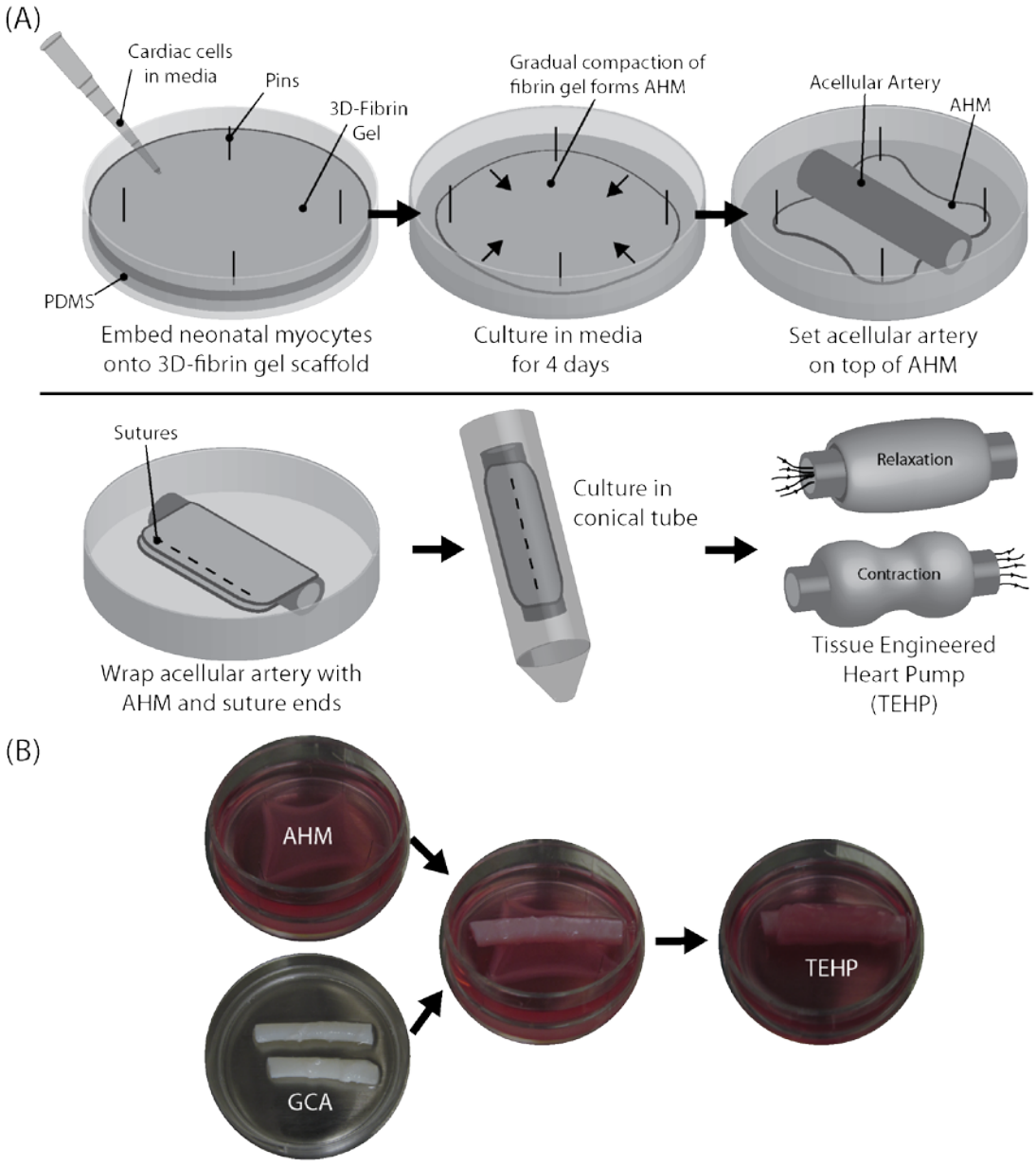

Figure 11. Methodology for fabrication of tissue engineered heart pumps (TEHPs). A) Schematic detailing the individual steps. B) Photographs of the artificial heart muscle and goat carotid artery form of the TEHP.

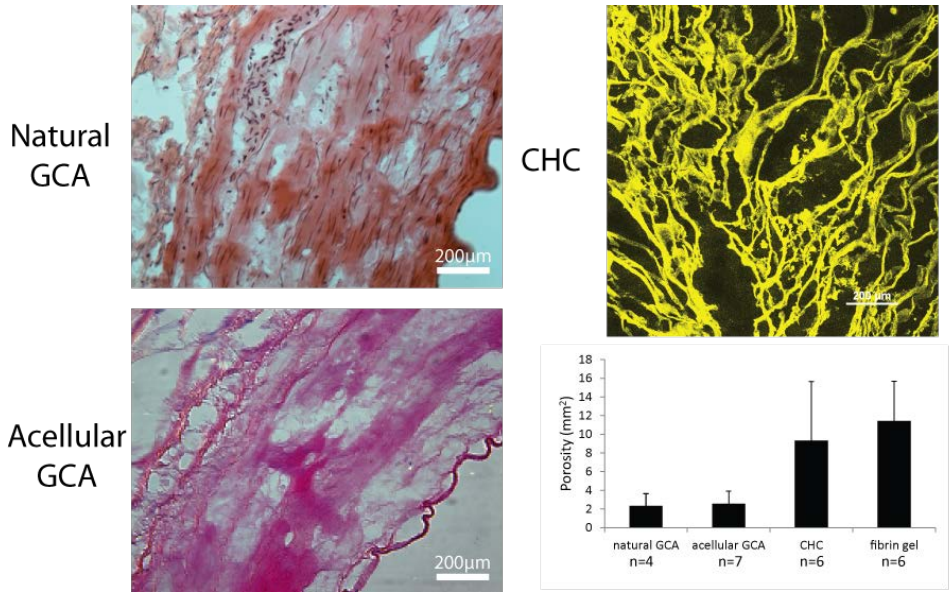

Figure 12. Tubular scaffold porosity for decellularized goat carotid arteries (GCAs) and chitosan hollow cylinders (CHCs) as compared to natural GCAs and fibrin gel.

5.2 Biopotentials for experimental TEHPs

Assessment of cardiomyocyte cell-to-cell interactions was performed by measurement of cardiac biopotential. A 32-electrode, in a 4 by 8 array, biopotential sensor was adapted to the PowerLab system used for twitch force recordings mentioned above. Biopotential readings were output as raw data from PowerLab and processed in MATLAB using a custom script. The raw data was scanned for segments of a periodic waveform in multiple channels, signifying a biopotential stimulus throughout the TEHP. The waveform in each channel may be out of phase, as expected for a conductive depolarization wave across the TEHP. Single AHM layer TEHP wrapped in both the distal and proximal configuration were tested for biopotential incidence.

Of the 32 electrodes equipped to the biopotential sensor, only 16 made complete contact with the TEHP. The data channels corresponding to these 16 electrodes were scanned for the presence of a biopotential. Figure 13 shows a representative biopotential

recording from 8 channels for a TEHP sample wrapped in a proximal configuration. The frequency of the sinusoidal waveform was ~2.5 Hz, matching the microscopic contractions observed under a stereo microscope, immediately before biopotential measurement.

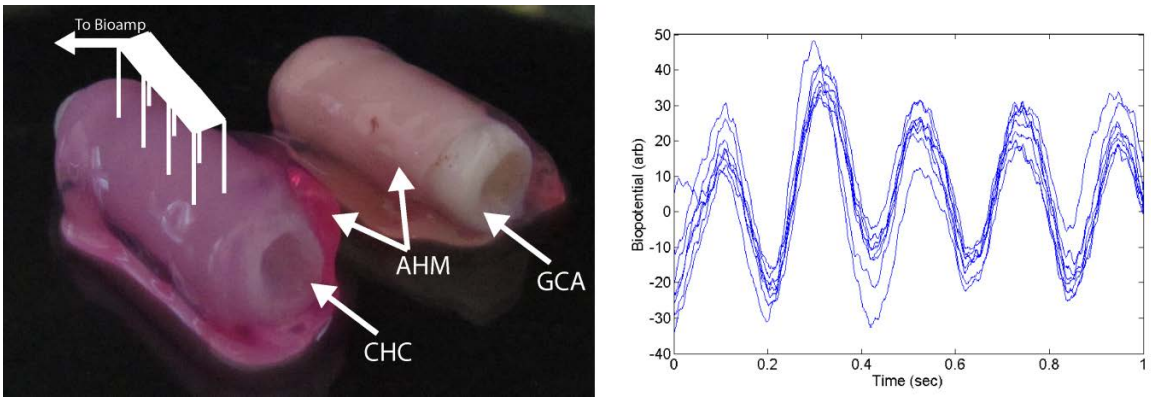

Figure 13. Biopotential measurements of TEHPs composed of CHC and GCA (left) and a representative plot from 8 electrodes showing the phase delay used to determine conduction velocities.

5.3 Cell injections versus AHM

The direct cell injection of cardiac cells resulted in a number of scattered cell clusters throughout the GCA and CHC scaffolds. Overall, cardiac cells within these sporadic clusters exhibited minimal expression of connexin43 and α-actinin. No contractions were observed for injected samples throughout culture. On the other hand, more expression of connexin43 and α-actinin was detected in TEHP samples formulated with an AHM. This comparison is observable in the representative immunohistochemistry slices, and holds true throughout the entire slice depth, as seen in the Figure 14 confocal z-stacks. No difference in comparing cell injection and AHM cell delivery mechanisms was found between GCA and CHC samples.

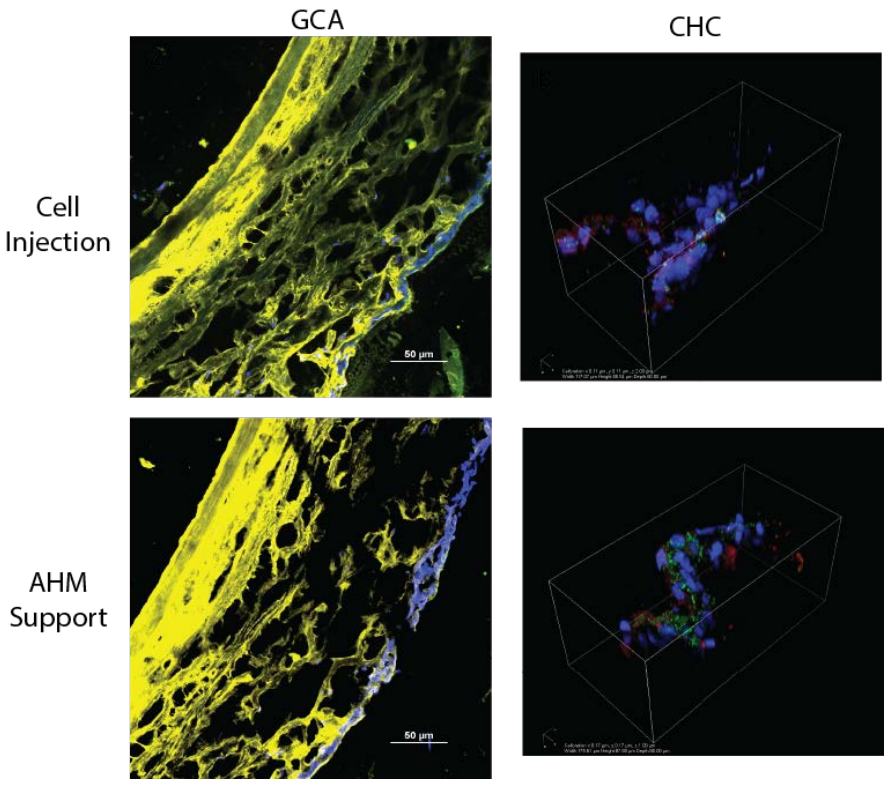

Figure 14. Cell injection vs AHM loading on GCA and CHC TEHPS. AHM more successfully transplanted cells to the periphery of GCAs and CHCs, while maintaining cardiac myocyte phenotype.

5.4 Proximal versus Distal AHM Configuration

The orientation of the cardiac cell layer on top of the AHM when wrapping around the GCA or CHC during TEHP formation had a significant effect on cell retention. AHM wrapped in the proximal configuration, with the cardiac cell layer wrapped adjacent to the GCA or CHC periphery, contained more cells on average. AHM wrapped in the distal configuration, with the cardiac cell layer exposed directly to the surrounding media, had a fewer number of scattered cell pockets around the TEHP. Figure 15 shows a representation of this distinction. However, TEHP formed in the distal configuration spontaneously contracted for a longer period of time in culture, and, in general, had more notable biopotentials.

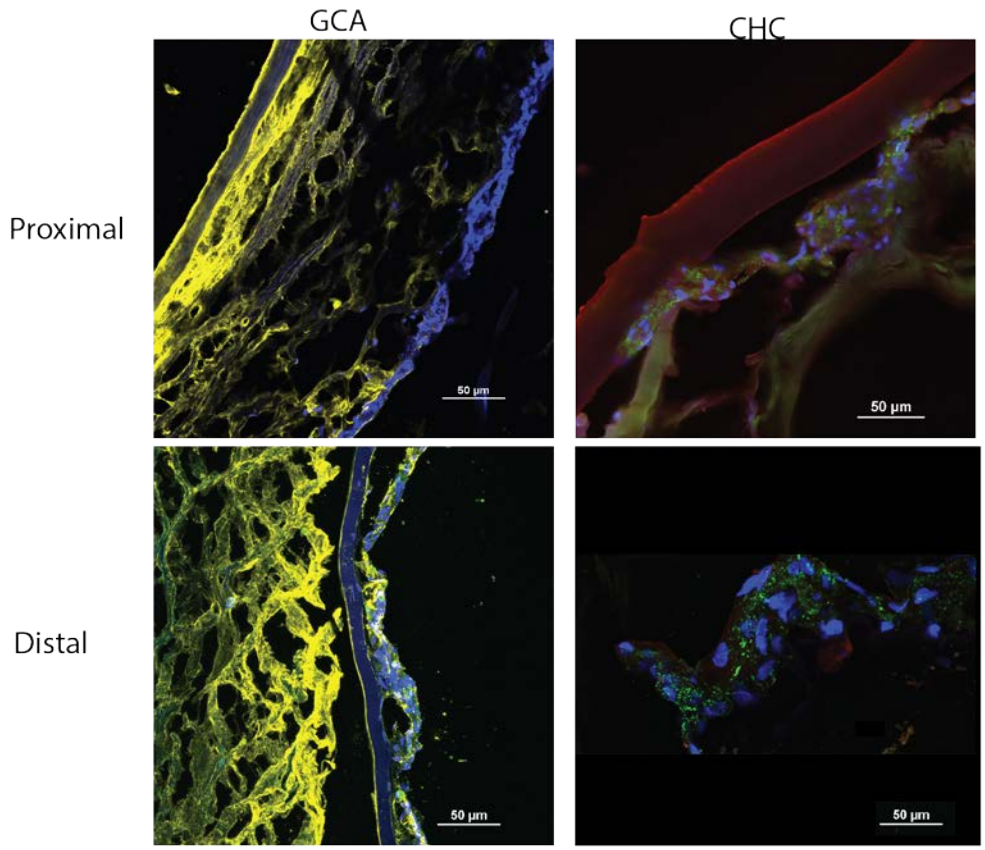

Figure 15. Proximal vs Distal TEHPs formed by either wrapping the AHM with cell side facing periphery of GCA or CHC, or with cell side facing immersion bath.

5.5 AHM Fibrin Gel Degradation versus Preservation

Cardiac cells naturally produce fibrinolysis enzymes capable of degrading the fibrin gel of the AHM. By taking advantage of this natural process, the fibrin gel can be used to temporarily provide the cardiac cells with a support matrix. After 8 days of culture, the fibrin gel fully degraded, allowing the cardiac cells to reside directly onto the GCA periphery.

The second method inhibited the degradation of the fibrin gel using aminocaproic acid, thus preserving its purpose as an intermediate scaffold between the cardiac cell layer and the surrounding culture media or the GCA and CHC. Masson's trichrome enabled a

clear distinction between the three scaffolding components of a TEHP; collagen and elastin of the GCA, the natural extracellular matrix (ECM) proteins produced by the cardiac fibroblasts on the AHM, and the fibrin gel composed of fibronectin. Immunostaining, shown in Figure 16, revealed an abundance of cells for the non-degraded fibrin gel methods. This method resulted in more notable formation of cardiac fibroblast-produced collagen and the expression of α-actinin by the cardiac myocytes. These naturally produced proteins adhered to both the fibrin gel and acellular GCA.

5.6 Bi-layer TEHP

Two layers of AHM were wrapped around an acellular GCA, with both AHM layers either in a proximal (cell-side in) or a distal (cell-side out) configuration to form a bi-layer TEHP. A single suture tie had to be made to hold the inner layer in place while wrapping the outer layer. Localized contraction within both layers, more prominent in the outer layer, was observed until 6 days after wrapping. Figure 17 shows the histological results for double AHM wrapped TEHP. The two AHM layers remained in contact concentrically throughout culture.

Cardiac cell clusters are abundant between the layers for both proximal and distal configurations, since each configuration results in a nestling of cells between the two AHM layers. The proximal configuration allowed for cardiac cell permeation into the GCA. Without fibrin gel degradation, which was inhibited using aminocaproic acid, the cardiac cells could not permeate into the GCA for the distal configuration. Histology also demonstrated in the majority of cases that, qualitatively, the cardiac cell layer was absent around much of the periphery of the distal configuration TEHP, as apparent in Figure 17.

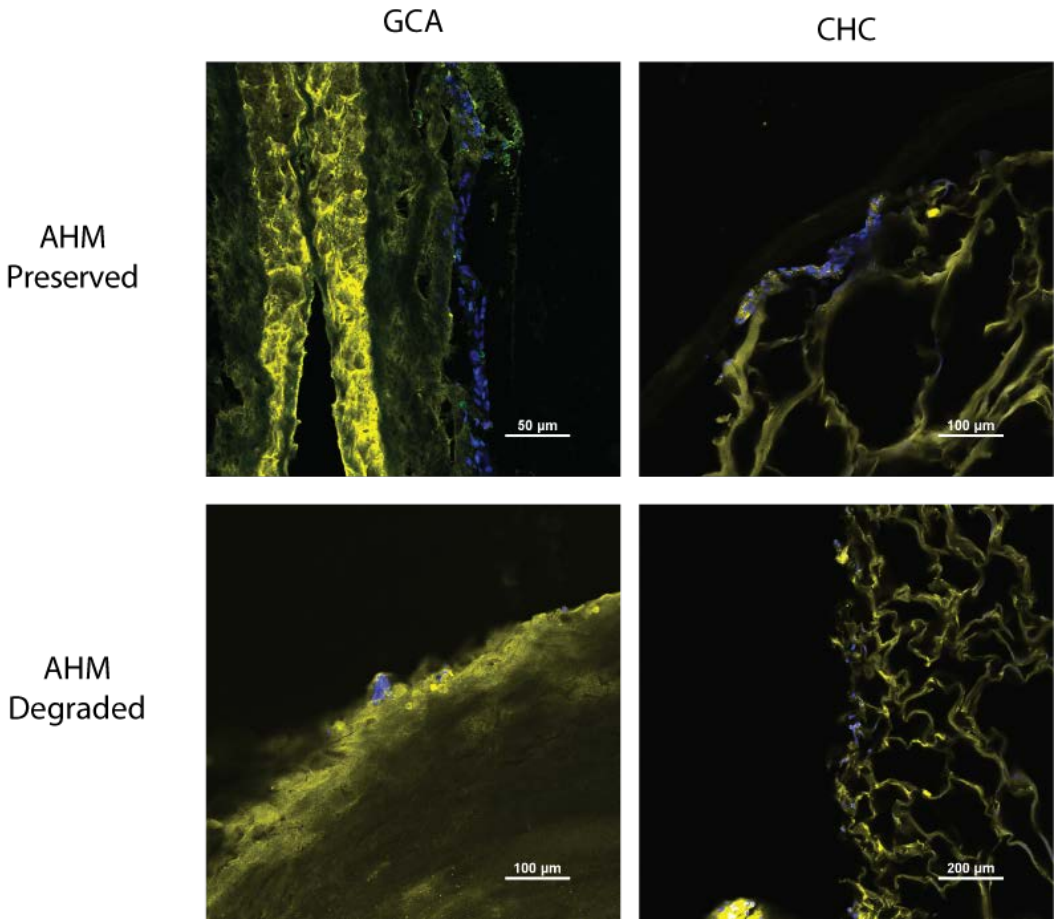

Figure 16. AHM was allowed to degrade by removing fibrinolysis inhibitor, EACA, to test ability to directly transplant cells to GCA or CHC periphery.

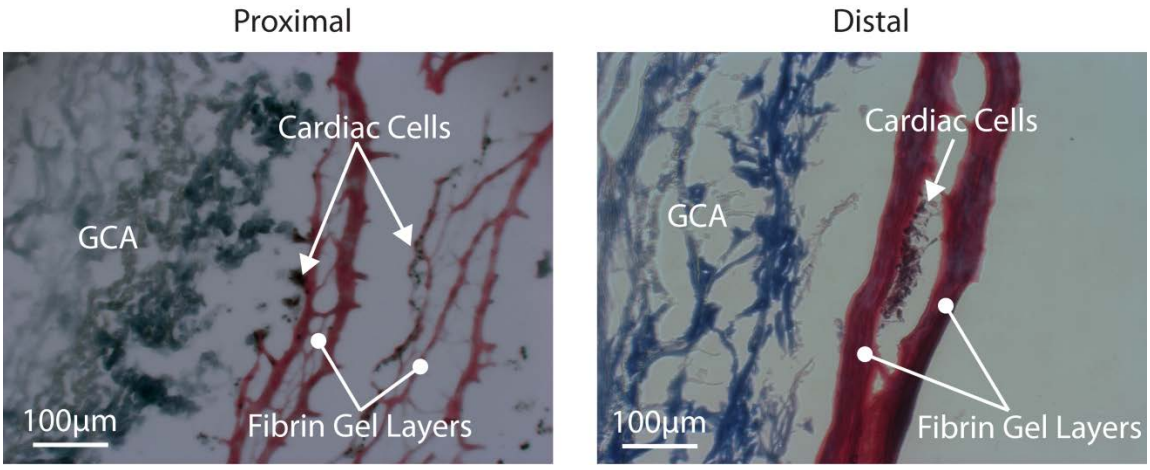

Figure 17. Double AHM with proximal and distal layering approaches for cell transplantation to GCA and CHC.

5.7 Experimental TEHP Verification

As a cell transplantation model, the AHM proved to be an effective tool for both the fibrin gel degradation and non-degradation methods. AHM composed of fibrin scaffolds employs the benefits of a natural, biocompatible, bioresorbable, and tunable polymer [70]. Fibrin has been used as a biological scaffold for stem and primary cells to regenerate cardiac, liver, nervous, ocular, and connective tissues [36]. Cardiac cell retention was achievable due to the natural adherence to fibronectin and use of proliferative neonatal cells [71]–[73]. Without the presence of a protease inhibitor (aminocaproic acid), the cells were able to degrade the fibrin gel [51]. As Figure 16 shows, the non-degraded proximal configuration resulted in, qualitatively, a higher cell-retention and GCA adherence. Use of a natural scaffold which is susceptible to cellular adhesion improves upon the lack of cell retention encountered in cell-seeding methods [74]. The histological evidence shown encourages further development of the TEHP, by the use of various

chemical and physical growth factors, and their assessment by quantifying cellular retention, organization, protein expression, and functionality.

For TEHP wrapped with AHM in a proximal configuration, cardiac cells resided on the surface of and were embedded within the GCA during culture (Figure 15). A few cells were able to penetrate through the vessel to the medial layer, approximately 60 μm from the GCA outer surface. Even though sustained contraction was not observed for these TEHPs, the presence of cells within the GCA layers demonstrated the viability of the cardiac fibroblasts. In contrast to the other cardiac cells, myocytes, smooth muscle, and endothelial cells, cardiac fibroblasts are more conducive to migration throughout natural extracellular matrices [75].

For TEHP wrapped in the distal configuration, the persistence of localized contraction suggested that cardiomyocytes were alive for at least 12 days after isolation from neonatal hearts. The presence of the fibrin gel, which was maintained by use of aminocaproic acid, inhibited cell migration into the GCA by acting as an impenetrable barrier to the cardiac cells. As a result, the cardiac cells maintained cohesive cell clusters on the fibrin gel, the outermost layer of the distally wrapped TEHP. In particular areas of the TEHP, only a single layer of cardiac cells was present. Whether this is a result of separation during culture or due to physical manipulation of the TEHP is unknown to us at the moment. Our primary goal moving forward is to maintain the initial multi-cardiac-cell layer, and, perhaps, even expanding on the number of layers by improving media perfusion into the inner layers.

Based on the greater presence of α-actinin (Figure 14), cardiac myocytes survival may have improved as a result of increased exposure to nutrients within the culture media.

Naturally, cardiac myocyte survival would lead to more interconnectivity between those cardiac myocytes. A key aspect of higher levels of interconnectivity is the presence of cell-produced ECM, which is evident in the histology shown in Figure 15.

Lack of pressure generation using the GCA scaffold may be a result of the thicker arterial tissue compared to the functional cardiac cell layer, ~1mm compared to ~50-100μm. It is this dimensional disparity which drove us to synthesis of CHC tubular scaffolds, of which we can control wall thickness and compliance. Although the CHC scaffold did not show as much cell retention or integration compared to the GCA, its structural integrity, porosity, and relative compliance make it an adequate candidate as a base component to a composite tubular scaffold. To improve cell integration, cardiac specific matrix proteins, such as collagen type I, collagen type IV, fibrin, and laminin, may be added into the chitosan base. In general, for both the GCA and CHC scaffolds, cardiomyocyte alignment should also be considered in order effectively utilize all of their contractile action.

Cardiomyocyte function may be enhanced by culturing TEHP in multi-stimulus bioreactors. Perfusion of media is pivotal in tissue engineering, and allows for homogenous distribution of nutrients, growth factors, ionic content, and molecular triggers. Mechanical stimulus by the use of pulsatile flow has been shown to control cardiomyocyte orientation and strengthen cell contraction. Electrical stimulation by current and frequency excitation of the cardiomyocyte depolarization wave has been shown to improve cardiomyocyte intercellular coupling and, thus, contraction synchronicity.

This work provided the initial step in identifying the advantage of using a support matrix as a cell delivery mechanism, as well as confirming the feasibility in maintaining

cardiac viability and functionality. Our next steps involve the use of these strategies to develop a functional TEHP capable of not only withstanding in vivo stresses, but also capable of generating transmural pressures. Optimization of cardiac function through the use of bioreactors may also bring functional TEHPs closer to reality. To determine if electrical stimulation can provide this enhancement, its effect on AHM function must first be assessed.

5.8 Electrical Stimulation of AHM

Electrical stimulation was applied to the contractile properties AHM through a custom build bioreactor capable of delivering stimulus to 6 AHM in 35mm dishes simultaneously, as shown in Figure 18. Three AHM are stimulated from a single channel output from a DAQ through 316 grade stainless steel electrodes spaced 5mm apart in each dish. The stainless steel electrodes do not make direct contact to the AHM, and are only submerged in the culture media. The circuit contains trichromatic LEDs to indicate delivery of stimulus to each well, with color, green for cathodic and blue for anodic wave, dictated by the direction of current allowed through the diodes. A 1kΩ resistor and a 10μF capacitor for each channel is added to further control the current and balance the charge delivered to the AHM. For the gene expression AHM, the stainless steel electrodes, spaced by 5mm, pierced the AHM from the bottom of the 16mm well and emerged through the medium.

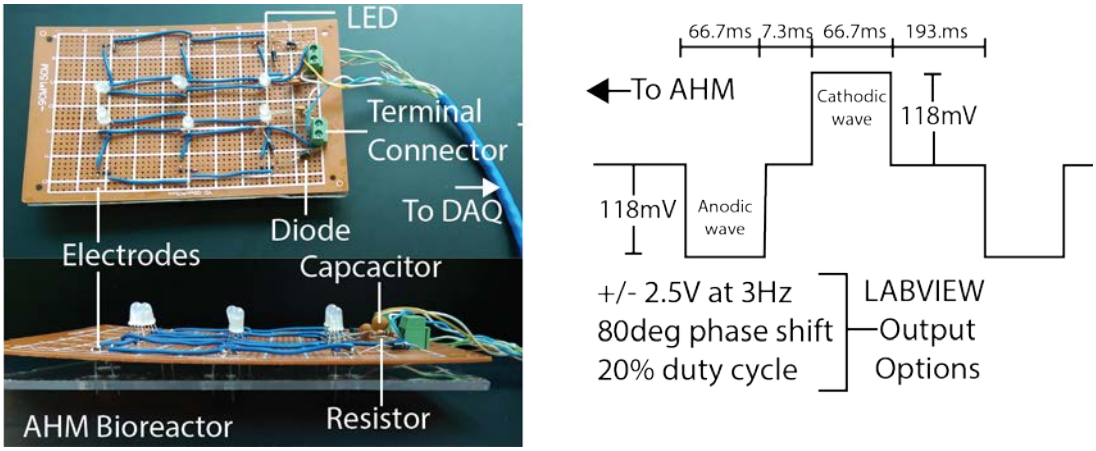

Figure 18. Electrical stimulation bioreactor for physiological experiments and for mini AHM used for gene expression analysis. AHM were stimulated with a biphasic waveform generated with LABVIEW.

Both AHM groups were stimulated with a biphasic square waveform, illustrated in Figure 18 as measured by an oscilloscope directly attached to the electrodes. In LABVIEW, two monophasic square waveforms of opposite polarity at + or - 2.5V, 3Hz, and 20% duty cycle were generated with an 80° phase shift and combined to form the biphasic wave. At the electrode spacing of 5mm, the electric field strength would thus be 5V/cm. The reason for using a 3Hz waveform, higher than the conventional 1Hz, is to elevate cardiac function of the AHM closer to the native rat heart of ~300bpm, without exhausting the cardiac myocytes in an oxygen poor culture environment. The 80° phase shift induces an interphase delay between the anodic and cathodic waves which improves threshold for stimulation and reduces the accumulation of deleterious Faradic reaction products [69].

This physically translates to a charge balanced biphasic wave with an interphase delay of ~10ms. The stimulus was intermittently delivered to the AHM in 30min intervals, separated by 30min rests, to encourage retention of spontaneous contractions. Preliminary studies showed that continuous stimulation inhibited spontaneous contractions in the

majority of ES AHM. A 30min rest time is also a means of further reducing the production of Faradic reaction products and electrode corrosion. Electrical stimulation was initiated at day 2 of culture.

5.8.1 Contractile Properties and Electrical Response

An optimized AHM can be characterized as having consistent twitch force output and rhythmic contraction. The effect of electrical stimulation on AHM twitch force output was observable in direct functional improvement. On the 6th day of culture, 4 days after initiation of electrical stimulation, electrically stimulated AHM had a significantly greater twitch force increase than control AHM, a difference which remained throughout culture up to day 12 (Figure 19).

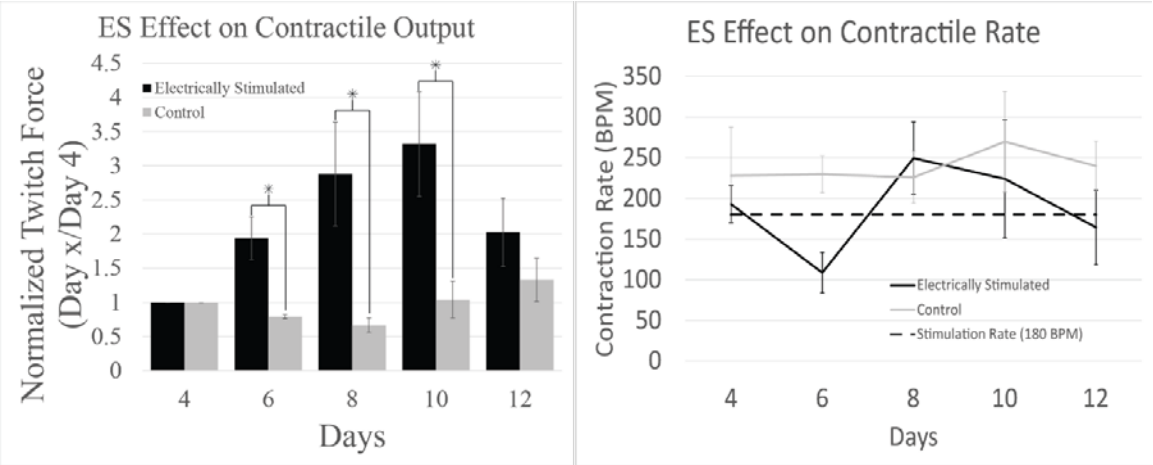

Figure 19. Normalized twitch force and contraction rate for control and ES AHM.

Electrically stimulated AHM was paced at a rate approximately half of a healthy resting rat's heart rate, ~360bpm [76]. This enabled us to more clearly determine if electrically stimulated AHM adapts to a pacing frequency during culture compared to the unstimulated control. The effect of electrical stimulation on AHM contraction rate is even

more profound. Electrically stimulated AHM contracted at rates that more closely hovered around 180bpm, the 3Hz electrical stimulation rate applied to the AHM during culture. The mean contraction rate was 291.7 ± 142.1bpm and 173.0 ± 63.2bpm throughout culture for control and electrically stimulated AHM, respectively. This indicates adaptation of the electrically stimulated AHM to the 3Hz pacing frequency. Number of samples used were n=18 for ES AHM and n=10 for control AHM.

The electrically stimulated AHM also had a significantly faster and more consistent response to a 1Hz pacing frequency during twitch force measurements. When stimulating the samples at 1Hz, the latency was 164.0 ± 38.2ms (n=10) and 100.1 ± 5.4ms (n=18) and for control and electrically stimulated AHM, respectively (Figure 20). Lower latency values imply improved cell junction coupling and conductivity of the AHM.

5.8.2 Cardiac Biopotential of ES AHM

To further evaluate the conductivity and the efficacy of electrical stimulation on improving electrophysiology of the AHM, we calculated the conduction velocity using a custom 32-electrode biopotential measurement system. By averaging the conduction velocity throughout the AHM, an assessment of the electrophysiological state of the AHM can be made. The conduction velocities on average were 15.4 ± 10.2cm/s (n=10) and 42.4 ± 13.8cm/s (n=18) for control and electrically stimulated AHM, respectively (Figure 20). The faster conduction velocities for electrically stimulated AHM correlates to the lower latency values obtained for the contractile response above. Both of these values signify more mature and well developed electrophysiological state for electrically stimulated AHM.

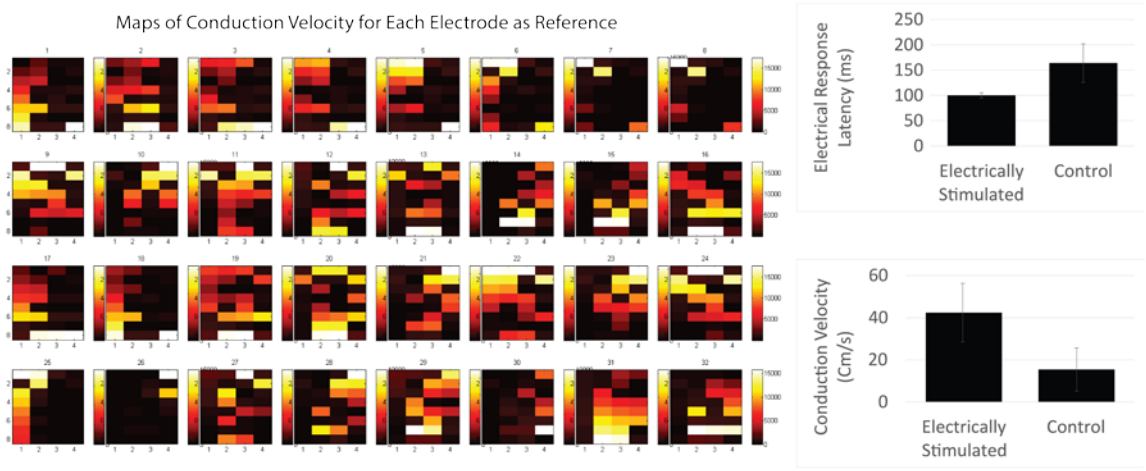

Figure 20. Biopotential conduction maps, conduction velocity, and Latency results for control and ES AHM.

5.8.3 Gene Expression of ES AHM

Relative expressions, illustrated in Figure 21 showed a peak at day 6 or 8 post-cell plating for the majority of the chosen genes. After the peak, relative expression was reduced to initial baseline values or slightly lower. The most dramatic change during the day 8 peak occurred for NAV1.5 and SCN7a, two voltage gated sodium channels. The lowest effect was for tnnt2, troponin T type 2, with a slight increase on day 6 and then a decrease to half of baseline levels by day 8. The only gene that immediately exhibited diminishing expression cav3.1, caveolin, which encodes for a protein component of a T type low voltage activated calcium channel.

5.8.4 Histological Assessment

Qualitatively, ES AHM segments fixed at day 12 and immunostained with connexin45 (cx45) and α-actinin showed higher fluorescence levels overall and improved sarcomere alignment and organization (Figure 22). Quantifying this representation using

relative signal volume indexes, as a ratio of the total measured signal from all fluorescence, showed higher expression of the key cardiac markers for ES AHM as compared to the controls. Measuring these ratios as the total volume of the observed field of view also indirectly showed increased cell presence, as evident by the higher DAPI volume index.

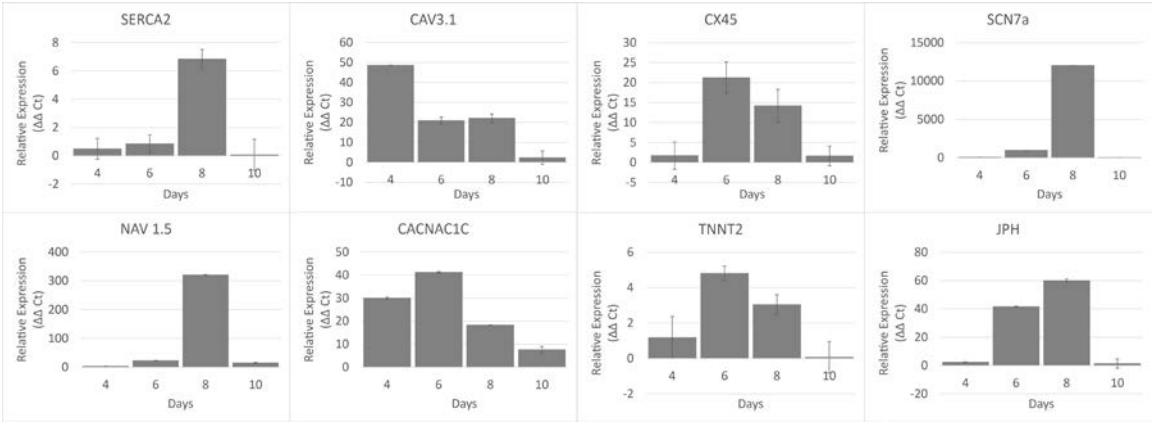

Figure 21. Relative gene expression throughout a 10 day culture after the onset of electrical stimulation normalized to GAPDH and control AHM.

5.8.5 ES AHM for Optimized TEHP

Electrical stimulation of pure myocyte cultures has a direct impact on function and physiology. Our results show that, on average, electrical stimulation of AHM will result in significant improvement of normalized twitch force within 48 hours of initiating the stimulus. Individually, however, control AHM are capable of spontaneous contractions that exceed the twitch forces of electrically stimulated AHM, particularly early on in culture. This is expected, since, electrical stimulation will not induce myocyte proliferation, but it may activate more myocytes to contract in unison more regularly. A more rhythmic and synchronous contractile AHM may induce positive genetic implications that result in a more optimized heart construct for tissue engineering research.

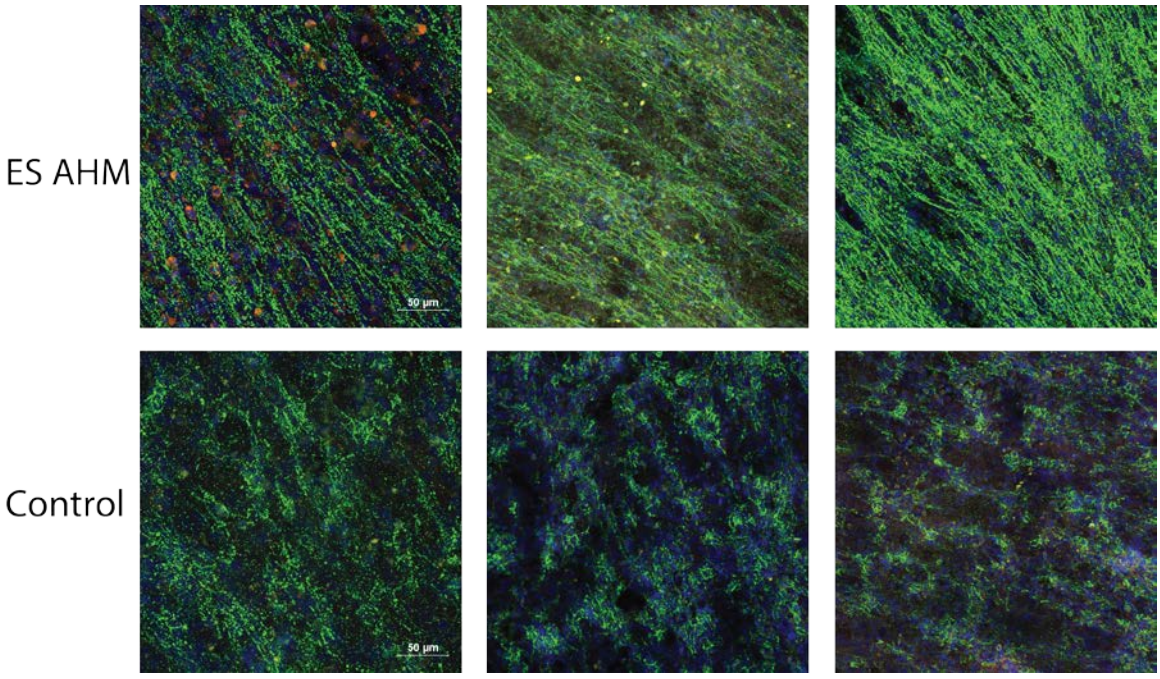

Figure 22. Histological assessment of α-actinin and connexin43 expression for control and ES AHM relative to nuclear staining with DAPI. ES AHM shows greater expression levels and improved alignment.

Previous studies have shown that electrical stimulation will increase contractile protein content and improve alignment, but the mechanism by which this occurs is unclear. Electrical stimulation may directly modulate gene expression, or it may operate indirectly via a mechanotransduction cascade activated by increased contraction [77][78]. What is clear is that ventricular myocytes that do not spontaneously contract, and that are not induced to depolarize by neighboring pacing cells, will now add to the functionality of the AHM. An active myocyte maintains its phenotype longer in culture, whereas an unstimulated myocyte has the tendency to undergo a dedifferentiation process in vitro [79].

Electrical stimulation for mixed cardiac cell cultures also facilitates adaptation to a prescribed external pulse rate and improves conduction velocity. These electrophysiology characteristics are vital for the maturation of the AHM and for its potential as an in vivo

support or repair construct for dysfunctional heart segments. The adaptation to the 3Hz electrical stimulation rate is evidenced by the improved linearity in measured contraction rate of 180bpm of the electrically stimulated AHM over the control AHM. A one-way ANOVA comparing the results of control and electrically stimulated AHM showed a p-value of 0.5351 for twitch force and 0.1261 for contraction rate. Although neither values show a significant difference between the ES and control groups, the lower p-value for contraction rate indicates that electrical stimulation may have more of an effect on contraction rate than on twitch force during the relatively short application period. A longer time frame may be necessary to achieve a significant difference in contraction rates and perhaps even twitch forces [80].

Improved conduction for electrically stimulated AHM was proven by two means in our study. We measured twitch force output of the AHM by either spontaneous or electrically stimulated contractions. For the electrically stimulated contractions, we measured the mean latency in the time required by the AHM to contract in response to the electrical stimulation. The latency values were significantly lower for the electrically stimulated AHM, which was 100.1 ± 5.4ms compared to the control at 164.0 ± 38.2ms. This result was reinforced by the conduction velocity measurements using our custom 32-electrode system. Electrically stimulated AHM had nearly 3 times higher mean conduction velocity than control AHM, Figure 20. This is an interesting result since natural conduction velocities within the whole heart range from 3-5m/s in Purkinje fibers to 0.5-1m/s in working ventricular myocytes. Electrical stimulation, as such, may have improved the development of a Purkinje fiber-like system within the AHM, resulting in the measured higher conduction velocity and lower latency.

The mechanism for improved AHM contractile regulation and electrophysiological condition may be elucidated from relative gene expressions. We have begun this investigation by selecting gene targets that regulate electrophysiological components, i.e. membrane or sarcoplasmic ion channels and cell-cell interaction regulators. The most significant change for the majority of the genes occurred at 6 or 8 days after the initiation of electrical stimulation. The genes that showed the most significant elevations at that time were Nav1.5 and SCN7a, which both code for voltage gated sodium channels. There is a strong correlation between elevated expression levels of signal transduction pathways and voltage gated ion channels and electrical stimulation, and our results support those findings [81]. The upregulation of cx45, a cardiac specific gap junction protein, was also significantly evident on day 6, and the histological assessment reinforces the translation of the cx45 sequences into functional protein.

The drop in expression levels for the majority of the genes at day 10 may be a result of fibroblast overgrowth. Since fibroblast proliferation is not controlled in our protocol, and myocyte proliferation is limited to a single division, if any, the effect on gene expression may by diluted by fibroblast RNA. The chosen genes should not be actively expressed in fibroblasts, and, likewise, may not be upregulated by electrical stimulation. The drop in expression levels, may also correlate to the drop in twitch force for both control and ES AHM at day 12. Further evaluation of these findings, by implementing strategies for controlling fibroblast growth, such as …, would shed light on this mystery.

To provide insight into the effects of electrical stimulation on the expression of genes coding for structural and contractile proteins, we selected tnnt2, a marker for troponin T type 2. The results showed a two-fold increase in expression at day 6, and a

steady decline to below baseline levels afterwards. We hypothesize that coupling electrical and mechanical stimulation, by applying an oscillating load, will more directly enhance the expression of tnnt2, as well as other structural and contractile proteins. This is already evident in the histological assessment of the α-actinin marker shows the resulting improved sarcomere organization and alignment relative to control AHM. The higher α-actinin signal volume index ratio for ES AHM reinforces this qualitative evaluation.

5.9 From Experimental Model of TEHP to Clinical Model

The experimental model of the TEHP verified a number of criteria for use of a more clinical formation as a biological CAD. First, cardiac cells were successfully transplanted from a multi-layer planar culture, to a more complex 3D-cylindrical shape, and cell viability was maintained for an extended culture time. Second, perfusion culture was adapted to facilitate cardio myocyte function without inducing atrophy or hypoxic conditions. Third, use of a tunable and biocompatible scaffold was found in chitosan, which with an abundant supply and ease of synthesis makes it an optimal biomaterial. Lastly, cardiac function was improved by use of an electrical stimulation bioreactor that not only improved cardiac function, but provided a means of producing more consistent and rhythmic AHM.

The next step now requires rebuilding the most important pillar of tissue engineering, the cell source. To make a truly human biocompatible and clinically relevant biological CAD option, use of rat neonatal cardiac cells must be replaced with a human cell source. For this aim, hADMSCs were differentiated through a process detailed in Chapter 2. This new cell source was seeded onto a chitosan-ECM hybrid scaffold to better

encourage cardiac differentiation and provide scaffold functionality and structural support. Use of bioreactors will then push the differentiation program even further towards a mature cardiac myocyte and results in a more clinically applicable TEHP.

6. Clinical TEHP Results

6.1 hADMSC Multi-step Programing towards Cardiac Progenitors

Trans-differentiation, which is the conversion of cell phenotypes by enhancement of particular gene expression, has gained a significant amount of attention and scrutiny [27], [82]–[86]. For the heart, the focus lies primarily on key transcription factors that spike during certain stages of cardiogenesis. A number of transcription factor combinations have been utilized, to convert primary cells into the cardiac lineage. Here, only two transcription factors, ETS2 and MESP1, were shown to initiate a program of trans-differentiation from hADMSC to an early hADCPs. Cells treated with ETS2 and MESP1 (EMA) were further matured through adrenergic stimulation by adding epinephrine to the culture media (EMAH). These cells were then cultured in a microgravity bioreactor to promote aggregation and hypoxic conditioning (EMAHR). The progression of cell maturity at each of these stages is shown in Figure 23, by expression of a key cardiac structural protein, αactinin, and a gap junction protein, connexin 43, used for cell signaling and conduction of the membrane potential depolarization wave.

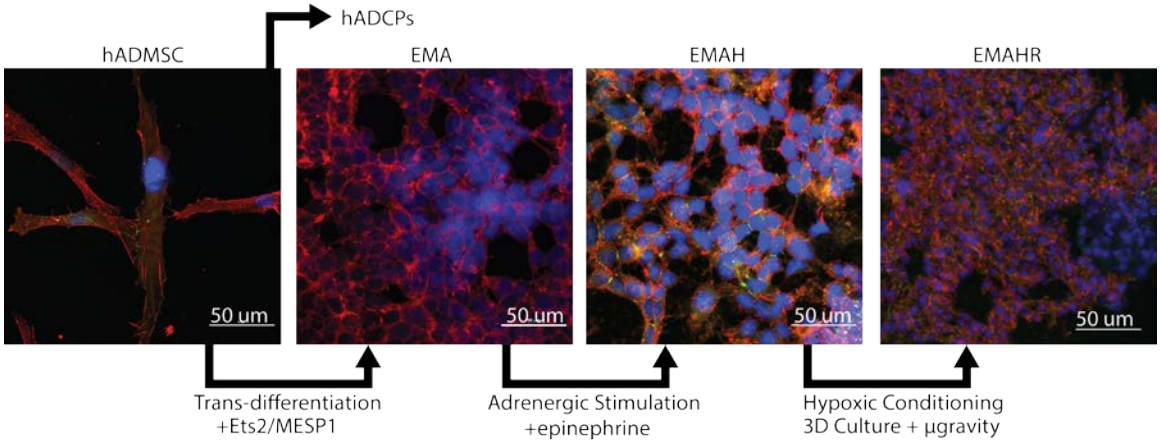

Figure 23. Trans-differentiation of hADMSC to hADCPs at different stages of the reprograming protocol with expression of αactinin (red) and connexin43 (green) and nuclear counterstaining with DAPI (blue).

During a six day time span within the rotating m, ADCPs coalesce to form cell aggregates. Within these aggregates, the cells undergo a hypoxic program that upregulates cardiac-specific genes for contractile proteins and ion channels, as revealed by PCR amplifications at specific time points during rotation (Figure 24). The upregulation of these genes may be a result of hypoxia inducible factor (HIF-1α/β), peroxisome proliferator-activated receptor c coactivator 1 (Pgc1α/β) and nitric oxide synthase (NOS) expression [87]–[91]. The induction of these pathways correlates to cardiogenesis of structural features of cardiomyocytes, and, more importantly for the integration of these cardiac progenitors with native tissue, key electrophysiological features, such as SR and t-tubule development.

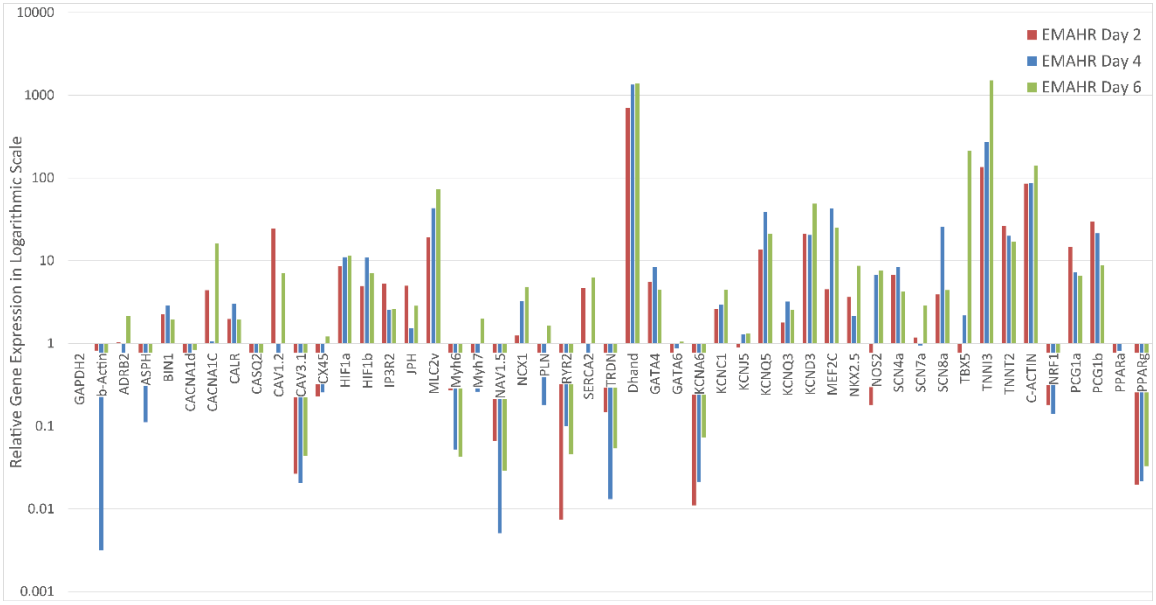

Figure 24. Relative gene expression of cardiac specific functions for hADCPs during the six day culture in a microgravity bioreactor (EMAHR) on a logarithmic scale normalized to the housekeeping gene GAPDH and hADMSC as control.

To identify the onset of the conduction system within the trans-differentiation program, cell samples at each stage were embedded within a fibrin gel and biopotential measurements were taken using the custom 32 electrode system. The biopotential data shown in Figure 25 represents electrical activity detected at 32 discrete and equally spaced electrodes. Each electrode's electrical activity is a measure of changes in voltage potential in reference to a common electrode placed in the media in which the cell-embedded fibrin gel is immersed. The number of amplitudes in the biopotential plots signify the level of electrical activity detected in each electrode. Amplitude patterns in the electrical activity is an indication of a polarization wave propagating across the detection region. The time delay between these mutual amplitudes can be analyzed using cross-correlation algorithms that, with the known distances between electrodes, result in a measure of the conduction velocity for the cell-fibrin gel construct.

A sign of cardiac cell precursor maturation is the increased electrical activity that is more widespread across the detection region. A higher number of amplitude patterns with less cross-electrode variation also showed the development of more conserved polarization waves. Higher conduction velocities imply improved cell-to-cell contact and gapjunction interactions. An additional explanation is that the high velocity and current modulation was also obtained due to the high expression of the hyperpolarization-activated and cyclic nucleotide-activated channel HCN1-4. Conduction velocities doubled to ~200mm/s after hypoxia induced maturation, and doubled yet again after dissociation of the 3D cell clusters for dispersion on top of the fibrin gel to ~400mm/s. By comparison normal conduction velocities within the whole heart range from 3-5m/s in Purkinje fibers to 0.5-1m/s in working ventricular myocytes.

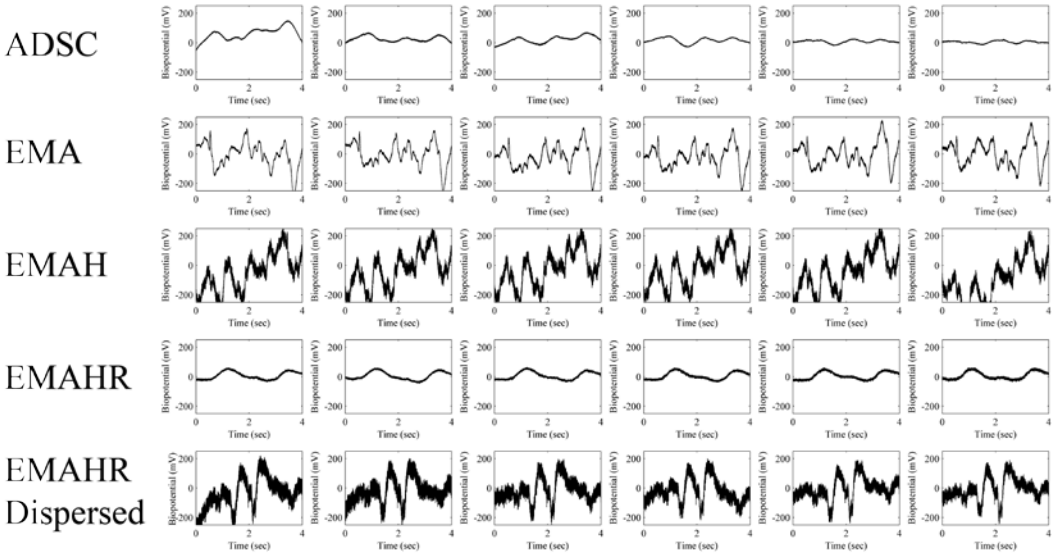

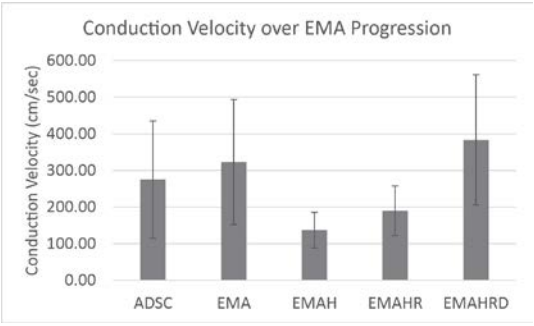

Figure 25. Biopotential recordings and conduction velocities from cells at the three stages of the trans-differentiation program embedded in fibrin gel.

The cells were also subjected to electrical stimulation to encourage expression of voltage gated ion channel and calcium handling proteins. A biphasic waveform used to stimulate 3D aggregates embedded in a fibrin gel. As shown in Figure 26, electrical stimulation further improved expression of adult myosin heavy chain gene (MHC-7, 1200-fold) to promote development of contractile myocytes progenitors. A number of other genes were also upregulated as a result of electrical stimulation via voltage-gated gene pathways. These genes included ADRB2 (20-fold stim, 15-fold non stim), ASPH (15-fold stim, 5-fold non-stim), BIN (10-fold stim, 5-fold non-stim), CACNA1C (25-fold stim, 30-

fold, non-stim), CALR (15-fold stim, 13-fold non-stim), CAV1.2 (18-fold stim,15-fold non-stim), HIF1a (70-fold stim, 45-fold non-stim), IP3R2 (15-fold stim, 2-fold non-stim), JPH (125-fold stim, 55-fold non-stim), MLC2v (135-fold stim, 70-fold non-stim), NCX1 (30-fold stim, 2-fold non-stim), PLN (10-fold stim, 20-fold non stim).

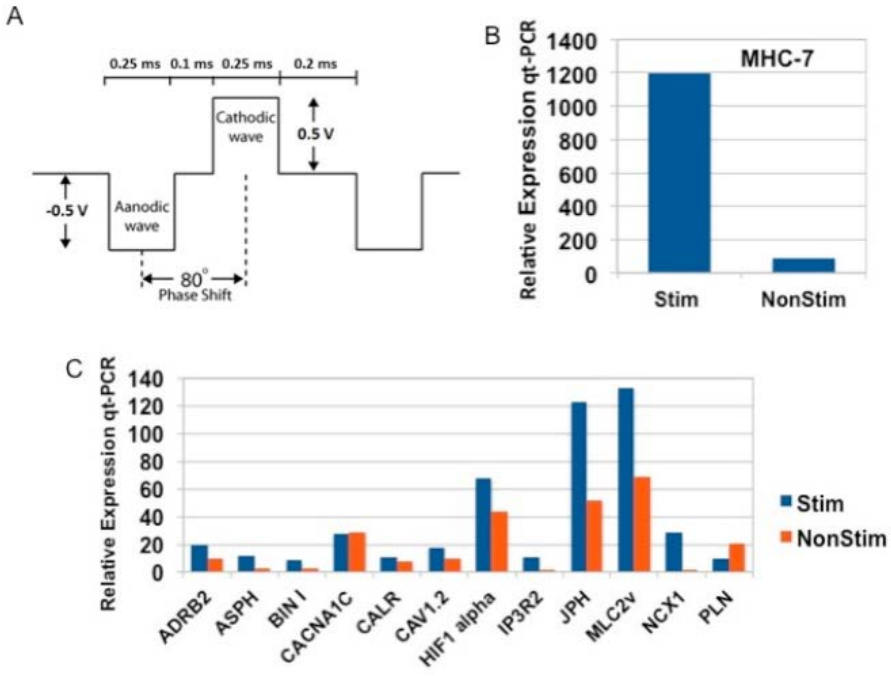

Figure 26. Electrical stimulation of EMAHR in fibrin gel improved expression of calcium handling proteins and structural proteins, such as myosin heavy chain-7 (MHC-7).

Maturation of the hADCP through adrenergic signaling, hypoxic conditioning, and electrical stimulation promote its applicability to a more clinically relevant TEHP. By culturing hADCP in a suitable biomaterial, its maturation can be progressed through use of pulsatile flow bioreactors, in conjunction with continued electrical stimulation.

6.2 Embedding hADCP in Chitosan-ECM Hybrid Scaffolds

As a final step to developing a model for TEHP, hADCP that have been reprogrammed from hADMSC through the three stage program outlined above, were cultured in chitosan-ECM hybrid scaffolds. The hybrid scaffolds were made by the synthesis of ECM-laden chitosan crosslinked sheets. The ECM has isolated from decellularized and processed porcine hearts. Chitosan-ECM scaffolds were ethanol sterilized and ultraviolet light treated overnight. The scaffolds were allowed to dry before loading with stage three EMAHR cells at a concentration of ~10^6 cells/ml, in order to promote optimal cell uptake by media absorbance. The chitosan-ECM scaffolds loaded with EMAHR cells, forming the TEHP construct, were then placed in the incubator for 1 hour without submersing in media, in order to encourage cell adhesion.

The TEHP constructs, were cultured in static conditions for 48 hours, before applying transferring them to a perfusion bioreactor shown in Figure 27. The perfusion bioreactor, since it is powered by a peristaltic pump, doubles as a low pressure pulsatile flow bioreactor, with pulse waves ranging from 5 to 15mmHg. The TEHP construct is suture tied at both ends to silicone tube inserts to attach to the bioreactor flow. Since the chitosan-ECM scaffold is highly porous, luminal flow is expected to permeate through the scaffold into the surrounding immersion bath. As such, the immersion bath and the luminal flow are connected to the same flow line to promote balance of the fluid exchange, and prevent overflow of the immersion bath.

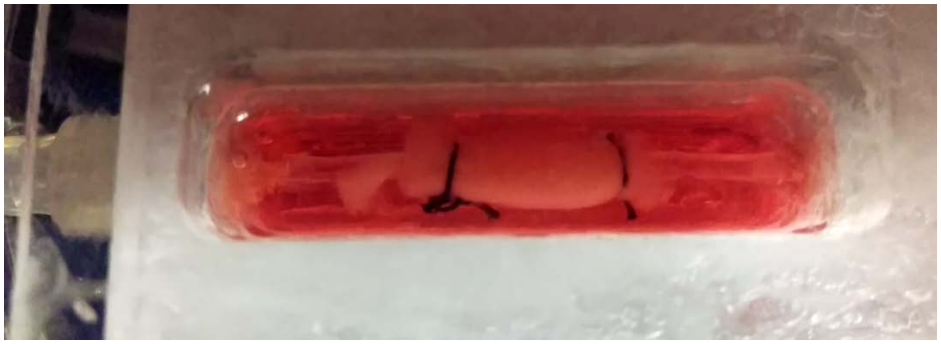

Figure 27. TEHP formed with chitosan-ECM scaffold and EMAHR cells in a perfusion/pulsatile flow bioreactor as the clinical TEHP model.

The construct was perfused for four days at a flow rate of 50 ml/min. At day four of culture, the construct was fixed and sectioned for histology to determine cell adhesion, retention, and proliferation throughout. The hematoxylin and eosin stain shown in Figure *28* revealed presence of nuclei, pertaining to cell locations, throughout the scaffold, as well as discrete zones of chitosan (light pink) and ECM (dark pink/red) components of the scaffold. This provides evidence for the efficacy of the simple cell seeding technique used, cell-suspension absorption, as well as retention of the cells during perfusion culture.

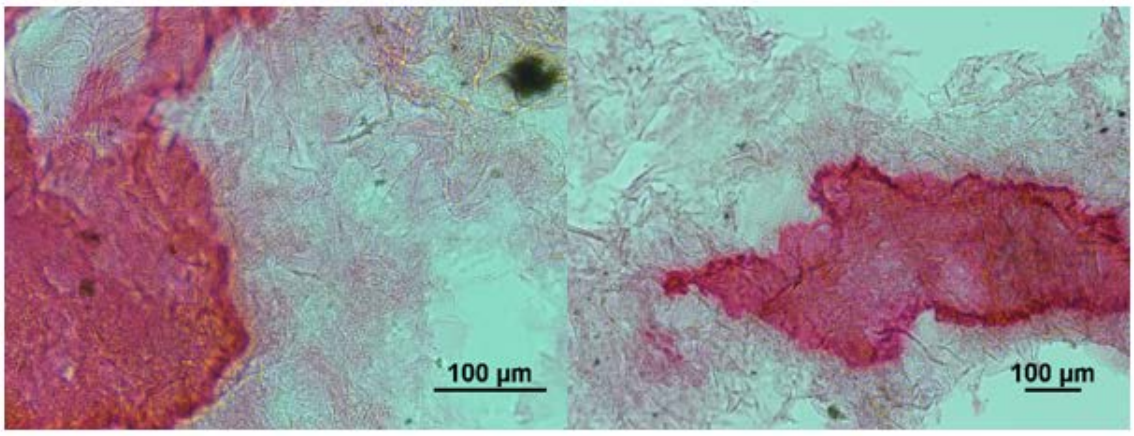

Figure 28. Hematoxylin and eosin stain of clincal model TEHP showing presence of cells (black) within the chitosan-ECM tissue. Light pink represents chitosan and dark pink/red represents ECM components of the scaffold.

Before histology was performed, a holding pressure test was performed on the clinical model TEHP, and results were compared to the experimental model TEHP. For the clinical model to be utilized in a pulsatile perfusion bioreactor, to provide the mechanical stimulus that will further encourage hADMSC reprogramming into cardiac progenitors, it must be able to hold intraluminal pressure during culture. The simple setup shown in Figure 29, where a syringe is used to pressurize the TEHP with inline flow and a terminal end, proved that the clinical TEHP model was able to inflate and hold pressure.

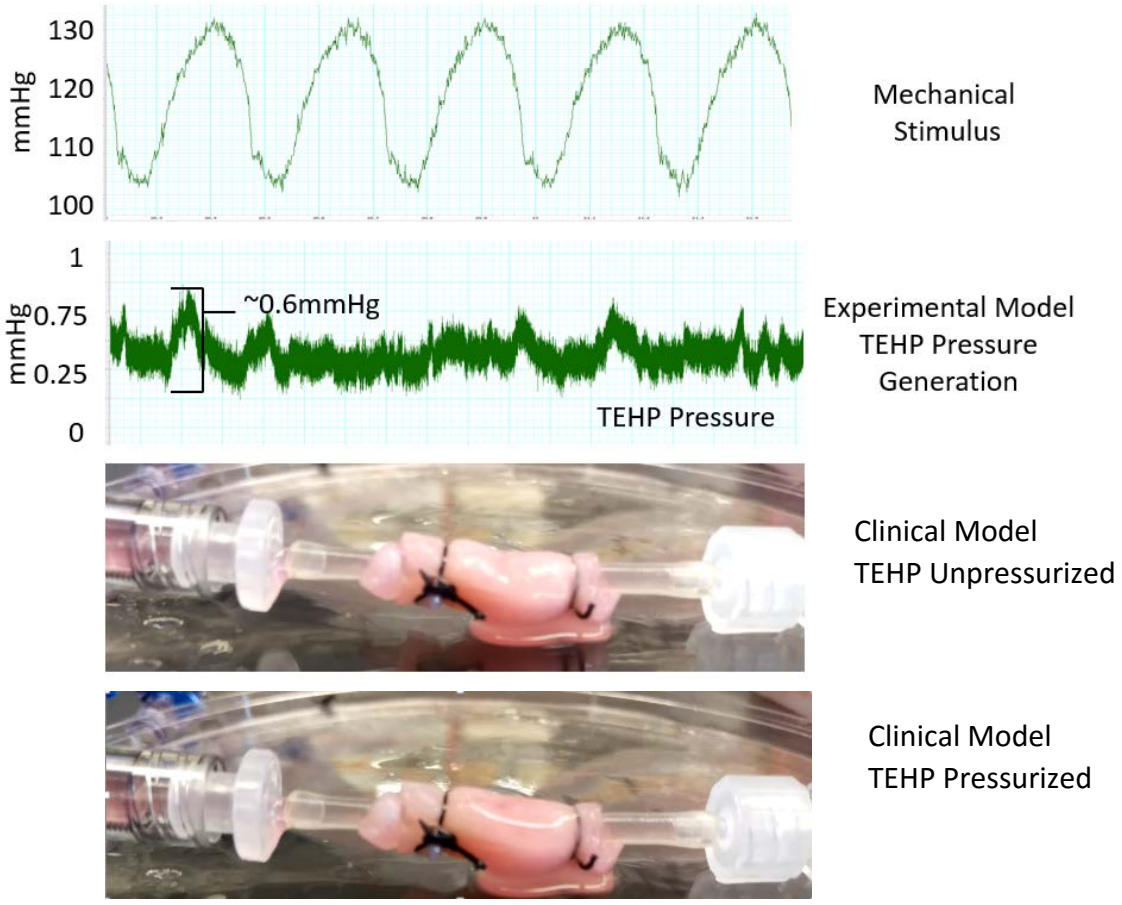

Figure 29. TEHP mechanical stimulus by pulsatile flow, expected pressure from experimental model, and pressure holding test for clinical model.

6.3 AHM for Assessment of Oxidative Stress on Cardiac Tissue

Reactive oxygen species (ROS) and their role in cardiovascular health have received clinical attention over the past decade. Atherogenesis, the development of plaque formation in the vascular wall, for instance, has been shown to be influenced by NAD(P)H oxidase-derived ROS within the vasculature [92]. A number of therapies, such as those used to treat chronic kidney disease, require erythropoiesis-stimulating agents. These therapies often include the use of intravenous iron to enhance effectiveness of erythropoiesis-stimulating agents. However, since iron is a transition metal and a potent pro-oxidant capable of producing ROS, administration of acute-high intravenous iron dose may reduce the forearm flow-mediated dilation in healthy individuals [93]. This has direct implications on cardiac load, and indirect implications on cardiac health.

To determine the direct effects of ROS on cardiac function in a more empirical manner, AHM optimization strategies and functional assessment were tested in the presence of ROS. Ferric chloride, the same source of iron used in intravenous iron therapies, was added to culture media at low (250µM) and high (750µM) concentrations. AHM were cultured in three groups, control, low, and high oxidative stress conditions. Twitch force measurements and histology was then performed to determine the effects on AHM functionality. Figure 30 shows the twitch force for the three groups. Each AHM was normalized to its baseline twitch force output generated at day 4. Control groups showed normal cardiac function improvement of ~1.5 times during culture. Low and high iron concentration groups showed progressively lower cardiac function over time, with statistical significance obtained between control and experimental groups obtained at day 10 of culture.

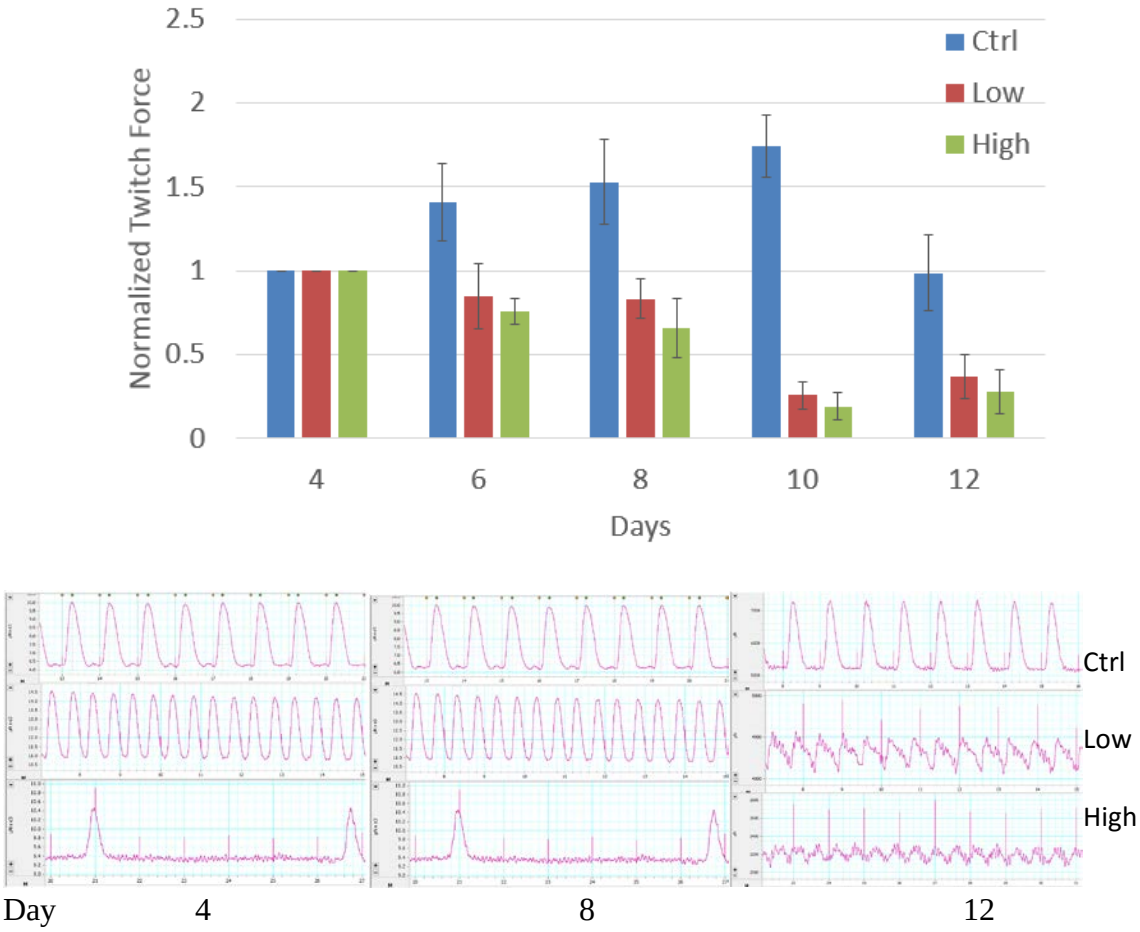

Figure 30. Normalized twitch force of control and oxidative stress AHM and representative plots at days 4, 8 and 12. Statistical significance ($p<0.05$) between control and experimental groups obtained at day 10 of culture.

Histology performed on AHM group revealed presence of intracellular iron uptake and oxidative stress. Brightfield images of AHM sections stained with H&E, for nucleic and ECM staining, and Prussian blue, for iron staining, showed the presence of iron in localized clusters residing within the cell membranes of cardiac cells residing in the cardiac layer on top of the fibrin gel. The effect of ferric chloride on the oxidative stress of the cardiac cells can be captured by the relative intensities of dihydroethidium (DHE), a superoxide indicator that intercalates within the cell's DNA. DHE normally fluoresces blue

until oxidized, staining the nucleus a bright red fluorescence, and the level of fluorescence can be an indirect measure of relative oxidation.

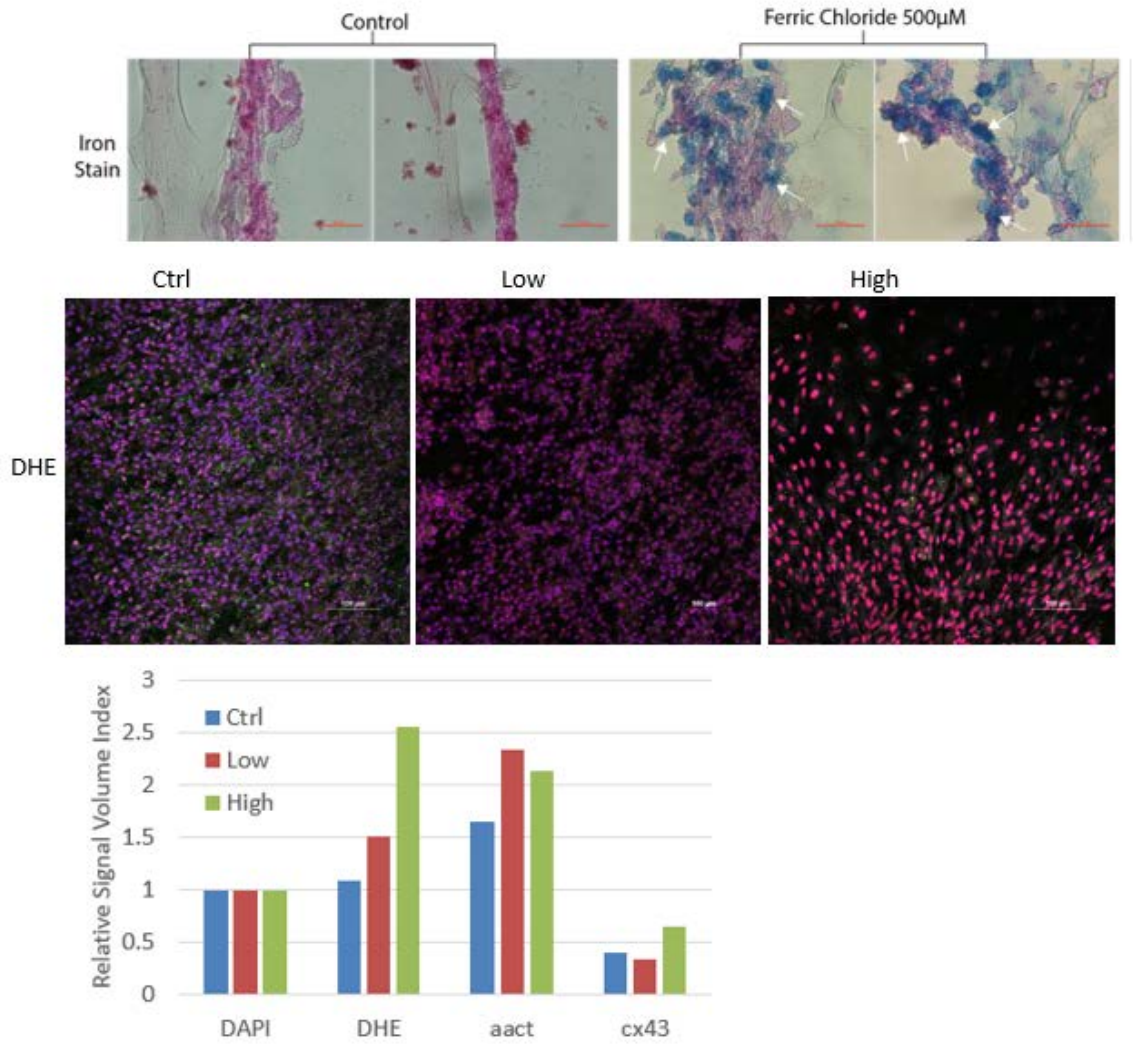

Figure 31. Top, Immunostains of DHE stained AHM for control, low, and high ferric chloride. Middle, control and oxidative stressed AHM loaded with 500µM ferric chloride. Bottom, relative signal volume index of control, low and high ferric chloride from immunostained z-stack volumes.

6.4 Crosslinked Gelatin Scaffolds

In an attempt to formulate a more structurally sound biomaterial for TEHP, gelatin, a denatured form of collagen, was synthesized by our collaborators. Gelatin was electrospun and crosslinked using hexafluoroisobutylene (Hfib), which allows for stability of the scaffold in culture, by reducing its degradation and providing for more elasticity. To characterize this mechanical advantage by crosslinking, tensile and compressive stress-strain analysis was performed using an Instron THE Model 5843 (Norwood, MA) on crosslinked samples hydrated in PBS at room temperature for at least 1 hour. Uncrosslinked samples were hydrated dropwise, since over hydration would disintegrate the scaffold. Samples prepared for tensile testing were 10 x 20 x 0.5 mm (width x length x thickness) and for compressive testing were 10mm in diameter and 1 mm thick. Rate of elongation and compression was 2 mm/min, starting at a preload of 0.02 N until 50% strain for tensile tests and until 90% strain for compressive tests. The Young's and compressive modulus were computed from the slope of the tensile and compressive stress-strain plots in the 0-5% and 0-10% strain region for tensile and compressive tests, respectively.

During elongation, uncrosslinked samples failed at high yield stress and low strains, and were stiff compared to crosslinked samples (Figure 32). Uncrosslinked samples also endured plastic deformation before failure. Crosslinked samples exhibited characteristics of a nonlinear elastic material until failure. In the physiological regime range of 0-10% strain, the mean Young's modulus was 382 ± 170 kPa (n=10) and 90 ± 52 MPa (n=6) for crosslinked and uncrosslinked samples, respectively. Representative stress-strian plots of uncrosslinked and crosslinked samples show transition from plasticity to elasticity after crosslinking gelatin. The compressive test resulted in a comparable mean compression

modulus of 254 ± 88 kPa (n=6) in the 0-10% strain (Figure 33). At a higher strain region of 0-20%, the mean elastic Young's modulus of 310 ± 121 kPa did not differ greatly compared to the lower strain range. Under a compressive load, however, the mean compressive modulus nearly tripled to 955 ± 403 kPa.

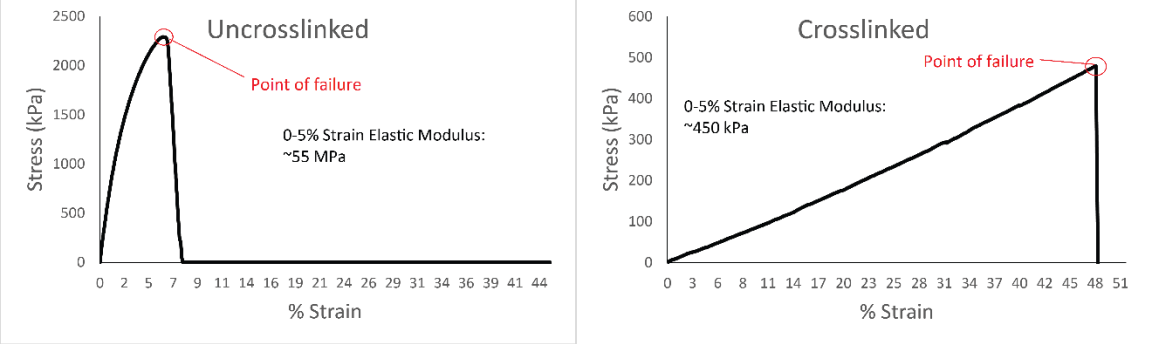

Figure 32. Representative tensile stress-strain plot within a 0-50% elongation strain region for uncrosslinked (left) and crosslinked (right) samples.

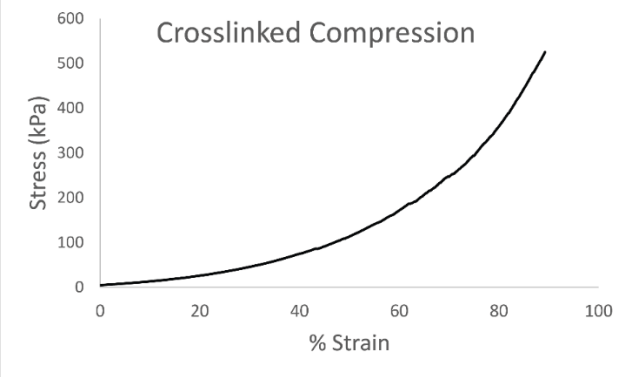

Figure 33. Representative compressive stress-strain plot within a 0-90% compressive strain region showing the nonlinearity of the material under a compressive load.

Soft-tissues are by nature nonlinear elastic materials. This means that under load, they are able to stretch and conform to a certain load, without damaging their structure. Nonlinear specifically means that there is no perfectly linear relationship between the amount of load applied and the amount of stretch or deformation that the tissue experiences. This nonlinear relationship exists for all soft-tissues in the body, such as cartilage and heart

tissue. A material follows a certain relationship between stress (load) and strain (stretch), until it fails, the point at which it tears or is unable to conform back to its original structure.

Now looking at the representative plots above, we can see the relationship between stress and strain of gelatin before and after crosslinking with Hfib. What you expect after crosslinking a material, is that you not necessarily make the material more rigid, but rather, more elastic. This is exactly the case for gelatin after crosslinking with Hfib. Before crosslinking, gelatin is stiff, experiencing a large amount of stress, >2MPa (2,000 KPa), and only stretching to ~7% its original length before failing. Collagen is inherently a very stiff material, in capable of deforming under load. It's what gives our body its structure and form, but it needs to be able to bend and deform under stress also. Crosslinking does just that. After crosslinking, gelatin only experiences ~500KPa, nearly 4 times less than before crosslinking, and is able to stretch to ~48% of its original length.

One thing you will notice also, is the shape of the plots. If we zoom in on a smaller region, you can see below that uncrosslinked gelatin has a plastic deformation plot shape (see example illustration below). Crosslinked gelatin, interestingly, actually showed a very linear stress-strain relationship. If you look at the R^2 value for each plot, crosslinked gelatin is much closer to a value of 1. This is not actually a bad thing, because most researchers model soft tissue dynamics using a linear relationship model, especially under low stress and strain (0 to 20% strain). Nonlinear relationship models are typically more accurate, especially for large strain application 50% or greater. Most elastic materials, such as a rubber band for instance, have linear behavior in low strain conditions, and exhibit nonlinear behavior under higher strains.

Preliminary culture of neonatal cardiac cells on crosslinked gelatin scaffolds showed retention of predominantly cardiac fibroblasts, and a few cardiomyocytes, as shown in Figure 34. SEM scans showed cell-matrix interaction along the fibers, yet, due to the high porosity of the scaffold fiber-fiber cell spanning and cardiomyocyte alignment was not observed. Nonetheless, this preliminary test shows promise for use of crosslinked electrospun gelatin with the cardiac progenitors detailed above. The porosity, of the scaffold will facilitate cell permeation into the scaffold, migration throughout, and space to proliferate. Since, gelatin is a denatured form of collagen, and the collagen used for this particular scaffold is bovine collagen type-1, the integrin profile of the cardiac progenitors will be optimally compatible for cell-scaffold binding. Preliminary studies have in fact proven that this scaffold proven was suitable in maintaining cell viability and even phenotype, of mesenchymal stem cells. We hypothesize that the same success will be obtained for the hADMSCs used to for reprogramming into cardiac progenitors.

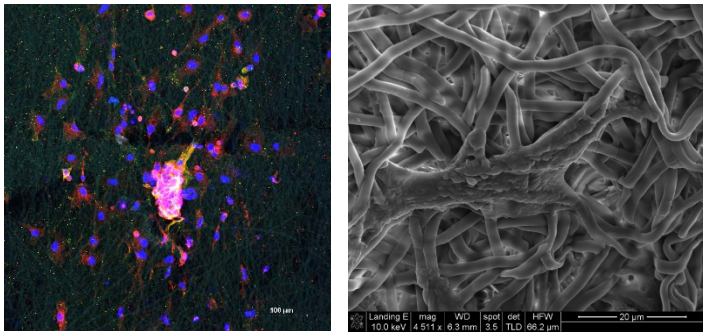

Figure 34. Immunostains (left) and SEM scans (right) of neonatal cardiomyocytes on top of gelatin scaffolds.

7. Conclusion

Development of a biological CAD has been assessed through the fabrication of a TEHP. An experimental model of a TEHP, utilizing rat primary cardiac cells as the cell source, showed the feasibility of culturing cardiac cells in a complex 3D environment, and tested the implementation of perfusion and pulsatile flow bioreactors. The model was then progressed towards a clinically applicable TEHP, by use of a human derived cell source, hADMSC, which has been trans-differentiated and matured towards a cardiac lineage progenitor, hADCP. The second generation TEHP was cultured in a biocompatible chitosan-ECM hybrid and conditioned with pulsatile flow and electrical stimulation. The lumen of the TEHP was also lined with human derived endothelial cells, to further facilitate its biocompatibility and reduce the potential for a thrombotic response.

Implementation of the TEHP may be as an inline support system, which replaces a segment of blood vessel in order to reduce the load downstream, and facilitate flow upstream. This study laid the foundation for the development of a natural alternative to CADs, which overcomes the disadvantages of current synthetic methods.

References

[1] M. A. Karsdal, F. Genovese, E. A. Madsen, T. Manon-Jensen, and D. Schuppan, “Collagen and Tissue Turnover as a Function of Age: Implications for Fibrosis,” *J. Hepatol.*, vol. 64, pp. 103–109, 2015.

[2] Z.-W. Tao, M. Mohamed, M. Hogan, B. Salazar, N. M. Patel, and R. K. Birla, “Establishing the Framework for Fabrication of a Bioartificial Heart,” *ASAIO J.*, vol. 61, no. 4, pp. 429–36, May 2015.

[3] A. J. Smith, F. C. Lewis, I. Aquila, C. D. Waring, A. Nocera, V. Agosti, B. Nadal-Ginard, D. Torella, and G. M. Ellison, “Isolation and characterization of resident endogenous c-Kit+ cardiac stem cells from the adult mouse and rat heart,” *Nat Protoc*, vol. 9, no. 7. pp. 1662–1681, 2014.

[4] B. S. Beltz, E. L. Cockey, J. Li, J. F. Platto, K. A. Ramos, and J. L. Benton, “Adult neural stem cells: Long-term self-renewal, replenishment by the immune system, or both,” *BioEssays*, vol. 37, no. 5, pp. 495–501, 2015.

[5] D. Mozaffarian, E. J. Benjamin, A. S. Go, D. K. Arnett, M. J. Blaha, M. Cushman, S. de Ferranti, J.-P. Després, H. J. Fullerton, V. J. Howard, M. D. Huffman, S. E. Judd, B. M. Kissela, D. T. Lackland, J. H. Lichtman, L. D. Lisabeth, S. Liu, R. H. Mackey, D. B. Matchar, D. K. McGuire, E. R. Mohler, C. S. Moy, P. Muntner, M. E. Mussolino, K. Nasir, R. W. Neumar, G. Nichol, L. Palaniappan, D. K. Pandey, M. J. Reeves, C. J. Rodriguez, P. D. Sorlie, J. Stein, A. Towfighi, T. N. Turan, S. S. Virani, J. Z. Willey, D. Woo, R. W. Yeh, and M. B. Turner, “Heart Disease and Stroke Statistics-2015 Update: A Report From the American Heart Association,” *Circulation*, vol. 131, no. 4, pp. e29–322, Dec. 2014.

[6] C. Engin, F. Ayik, E. Oguz, B. Eygi, T. Yagdi, S. Karakula, and M. Ozbaran, "Ventricular assist device as a bridge to heart transplantation in adults," *Transplant. Proc.*, vol. 43, no. 3, pp. 927–30, Apr. 2011.

[7] L. H. Cohn, "The role of mechanical devices," *J. Card. Surg.*, vol. 5, no. 3 Suppl, pp. 278–81, Sep. 1990.

[8] O. H. Frazier, "New technologies in the treatment of severe cardiac failure: the Texas Heart Institute experience," *Ann. Thorac. Surg.*, vol. 59, no. 2 Suppl, pp. S31–7; discussion S38, Feb. 1995.

[9] C. Cereghetti, C. Kaiser, and S. Cook, "Ventricular assist devices in acute heart failure," *Minerva Cardioangiol.*, vol. 60, no. 4, pp. 395–403, Aug. 2012.

[10] H. J. Evans, J. K. Sweet, R. L. Price, M. Yost, and R. L. Goodwin, "Novel 3D culture system for study of cardiac myocyte development," *Am J Physiol Hear. Circ Physiol*, vol. 285, no. 2, pp. H570–H578, 2003.

[11] M. J. Yost, C. F. Baicu, C. E. Stonerock, R. L. Goodwin, R. L. Price, J. M. Davis, H. Evans, P. D. Watson, C. M. Gore, J. Sweet, L. Creech, M. R. Zile, and L. Terracio, "A novel tubular scaffold for cardiovascular tissue engineering," *Tissue Eng.*, vol. 10, no. 1–2, pp. 273–284, 2004.

[12] H. Kubo, T. Shimizu, M. Yamato, T. Fujimoto, and T. Okano, "Creation of myocardial tubes using cardiomyocyte sheets and an in vitro cell sheet-wrapping device," *Biomaterials*, vol. 28, no. 24, pp. 3508–16, Aug. 2007.

[13] P. Menasche, "Cardiac cell therapy: Lessons from clinical trials," *J. Mol. Cell. Cardiol.*, vol. 50, no. 2, pp. 258–265, 2011.

[14] A. Abdel-latif, R. Bolli, I. M. Tleyjeh, V. M. Montori, E. C. Perin, C. A. Hornung,

E. K. Zuba-Surma, M. Al-Mallah, and B. Dawn, “Adult Bone Marrow–Derived Cells for Cardiac Repair,” *Arch. Intern. Med.*, vol. 167, pp. 989–997, 2007.

[15] M. Y. Emmert, R. W. Hitchcock, and S. P. Hoerstrup, “Cell therapy, 3D culture systems and tissue engineering for cardiac regeneration,” *Adv. Drug Deliv. Rev.*, vol. 69–70, pp. 254–269, 2014.

[16] V. F. M. Segers and R. T. Lee, “Stem-cell therapy for cardiac disease,” *Nature*, vol. 451, no. 7181, pp. 937–42, 2008.

[17] P. Ahuja, P. Sdek, and R. W. Maclellan, “Cardiac Myocyte Cell Cycle Control in Development, Disease and Regeneration,” *Physiol. Rev.*, vol. 87, no. 2, pp. 521–544, 2007.

[18] Y.-C. Huang, L. Khait, and R. K. Birla, “Contractile three-dimensional bioengineered heart muscle for myocardial regeneration,” *J. Biomed. Mater. Res. A*, vol. 80, no. 3, pp. 719–31, Mar. 2007.

[19] P. Menasché, “Embryonic stem cells for severe heart failure: Why and how,” *J. Cardiovasc. Transl. Res.*, vol. 5, no. 5, pp. 555–565, 2012.

[20] P. Dixit and R. Katare, “Challenges in identifying the best source of stem cells for cardiac regeneration therapy,” *Stem Cell Res. Ther.*, vol. 6, no. 1, p. 26, 2015.

[21] L. Barad, R. Schick, N. Zeevi-Levin, J. Itskovitz-Eldor, and O. Binah, “Human Embryonic Stem Cells vs Human Induced Pluripotent Stem Cells for Cardiac Repair,” *Can. J. Cardiol.*, vol. 30, no. 11, pp. 1279–1287, 2014.

[22] M. F. Pittenger, A. M. Mackay, S. C. Beck, R. K. Jaiswal, R. Douglas, J. D. Mosca, M. A. Moorman, D. W. Simonetti, S. Craig, and D. R. Marshak, “Multilineage potential of adult human mesenchymal stem cells,” *Science*, vol.

284, no. 5411, pp. 143–7, 1999.

[23] Y. Zhu, T. Liu, K. Song, B. Jiang, X. Ma, and Z. Cui, “Collagen-chitosan polymer as a scaffold for the proliferation of human adipose tissue-derived stem cells,” *J. Mater. Sci. Mater. Med.*, vol. 20, no. 3, pp. 799–808, 2009.

[24] C. Valina, K. Pinkernell, Y. H. Song, X. Bai, S. Sadat, R. J. Campeau, T. H. Le Jemtel, and E. Alt, “Intracoronary administration of autologous adipose tissue-derived stem cells improves left ventricular function, perfusion, and remodelling after acute myocardial infarction,” *Eur. Heart J.*, vol. 28, no. 21, pp. 2667–2677, 2007.

[25] J. M. Gimble, A. J. Katz, and B. A. Bunnell, “Adipose-derived stem cells for regenerative medicine,” *Circ. Res.*, vol. 100, no. 9, pp. 1249–1260, 2007.

[26] A. Schäffler and C. Büchler, “Concise Review: Adipose Tissue-Derived Stromal Cells-Basic and Clinical Implications for Novel Cell-Based Therapies,” *Stem Cells*, vol. 25, no. 4, pp. 818–827, 2007.

[27] J. F. Islas, Y. Liu, K.-C. Weng, M. J. Robertson, S. Zhang, a. Prejusa, J. Harger, D. Tikhomirova, M. Chopra, D. Iyer, M. Mercola, R. G. Oshima, J. T. Willerson, V. N. Potaman, and R. J. Schwartz, “Transcription factors ETS2 and MESP1 transdifferentiate human dermal fibroblasts into cardiac progenitors,” *Proc. Natl. Acad. Sci.*, vol. 109, no. 32, pp. 13016–13021, 2012.

[28] I. C. Scott, *Life Before Nkx2.5. Cardiovascular Progenitor Cells: Embryonic Origins and Development*, vol. 100. Elsevier Inc., 2012.

[29] J. Liu, D. K. Lieu, C. W. Siu, J. Fu, H. Tse, and R. A. Li, “Facilitated maturation of Ca 2 *2* handling properties of human embryonic stem cell-derived

cardiomyocytes by calsequestrin expression," pp. 152–159, 2009.

[30] M. C. Michel, S. E. Harding, and R. a Bond, "Are there functional β □ adrenoceptors in the human heart," *Br. J. Pharmacol.*, vol. 162, no. 4, pp. 817–822, 2011.

[31] D. Grimm, M. Wehland, J. Pietsch, G. Aleshcheva, P. Wise, J. van Loon, C. Ulbrich, N. E. Magnusson, M. Infanger, and J. Bauer, "Growing Tissues in Real and Simulated Microgravity: New Methods for Tissue Engineering," *Tissue Eng. Part B Rev.*, vol. 20, no. 6, pp. 555–566, 2014.

[32] M. Rienks, A. P. Papageorgiou, N. G. Frangogiannis, and S. Heymans, "Myocardial extracellular matrix: An ever-changing and diverse entity," *Circ. Res.*, vol. 114, no. 5, pp. 872–888, 2014.

[33] A. K. Capulli, L. A. MacQueen, S. P. Sheehy, and K. K. Parker, "Fibrous scaffolds for building hearts and heart parts," *Adv. Drug Deliv. Rev.*, vol. 96, pp. 83–102, 2016.

[34] M. J. Kocica, A. F. Corno, F. Carreras-Costa, M. Ballester-Rodes, M. C. Moghbel, C. N. C. Cueva, V. Lackovic, V. I. Kanjuh, and F. Torrent-Guasp, "The helical ventricular myocardial band: global, three-dimensional, functional architecture of the ventricular myocardium," *Eur. J. Cardio-thoracic Surg.*, vol. 29, no. SUPPL. 1, 2006.

[35] S. Fleischer and T. Dvir, "Tissue engineering on the nanoscale: Lessons from the heart," *Curr. Opin. Biotechnol.*, vol. 24, no. 4, pp. 664–671, 2013.

[36] T. A. E. Ahmed, E. V Dare, and M. Hincke, "Fibrin: a versatile scaffold for tissue engineering applications," *Tissue Eng. Part B. Rev.*, vol. 14, no. 2, pp. 199–215,

Jun. 2008.

[37] J. V. Quinn, *Tissue Adhesives in Clinical Medicine, Volume 1*. PMPH-USA, 2005.

[38] J. von Byern and I. Grunwald, Eds., *Biological Adhesive Systems*. Vienna: Springer Vienna, 2010.

[39] E. J. Cohn, L. E. Strong, W. L. Hughes, D. J. Mulford, J. N. Ashworth, M. Melin, and H. L. Taylor, "Preparation and Properties of Serum and Plasma Proteins. IV. A System for the Separation into Fractions of the Protein and Lipoprotein Components of Biological Tissues and Fluids 1a,b,c,d," *J. Am. Chem. Soc.*, vol. 68, no. 3, pp. 459–475, Mar. 1946.

[40] A. C. Brown and T. H. Barker, "Fibrin-based biomaterials: Modulation of macroscopic properties through rational design at the molecular level," *Acta Biomater.*, Sep. 2013.

[41] M. M. Martino, M. Mochizuki, D. A. Rothenfluh, S. A. Rempel, J. A. Hubbell, and T. H. Barker, "Controlling integrin specificity and stem cell differentiation in 2D and 3D environments through regulation of fibronectin domain stability," *Biomaterials*, vol. 30, no. 6, pp. 1089–1097, Feb. 2009.

[42] I. Catelas, N. Sese, B. M. Wu, J. C. Y. Dunn, S. Helgerson, and B. Tawil, "Human mesenchymal stem cell proliferation and osteogenic differentiation in fibrin gels in vitro," *Tissue Eng.*, vol. 12, no. 8, pp. 2385–96, Aug. 2006.

[43] G. Zhang, X. Wang, Z. Wang, J. Zhang, and L. Suggs, "A PEGylated fibrin patch for mesenchymal stem cell delivery," *Tissue Eng.*, vol. 12, no. 1, pp. 9–19, Jan. 2006.

[44] N. F. Huang, A. Lam, Q. Fang, R. E. Sievers, S. Li, and R. J. Lee, "Bone marrow-

derived mesenchymal stem cells in fibrin augment angiogenesis in the chronically infarcted myocardium," *Regen. Med.*, vol. 4, no. 4, pp. 527–38, Jul. 2009.

[45] A. Takei, Y. Tashiro, Y. Nakashima, and K. Sueishi, "Effects of fibrin on the angiogenesis in vitro of bovine endothelial cells in collagen gel," *In Vitro Cell. Dev. Biol. Anim.*, vol. 31, no. 6, pp. 467–72, Jun. 1995.

[46] R. K. B. Ze-Wei Tao, Mohamed Mohamed, Matthew Hogan, Laura Gutierrez, "Optimizing a spontaneous contraction heart tissue patch by seeding neonatal rat cardiac cells on fibrin gel," *J. Tissue Eng. Regen. Med.*, 2013.

[47] M. N. Hirt, A. Hansen, and T. Eschenhagen, "Cardiac tissue engineering: state of the art," *Circ. Res.*, vol. 114, no. 2, pp. 354–67, Jan. 2014.

[48] K. Uehara, C. Zhao, A. Gingery, A. R. Thoreson, K.-N. An, and P. C. Amadio, "Effect of Fibrin Formulation on Initial Strength of Tendon Repair and Migration of Bone Marrow Stromal Cells in Vitro," *J. Bone Joint Surg. Am.*, vol. 97, no. 21, pp. 1792–8, Nov. 2015.

[49] K. C. Murphy and J. K. Leach, "A reproducible, high throughput method for fabricating fibrin gels," *BMC Res. Notes*, vol. 5, no. 1, p. 423, 2012.

[50] J. D. Griffin and L. Ellman, "Epsilon-aminocaproic acid (EACA)," *Semin. Thromb. Hemost.*, vol. 5, no. 1, pp. 27–40, Jan. 1978.

[51] L. Kupcsik, M. Alini, and M. J. Stoddart, "Epsilon-aminocaproic acid is a useful fibrin degradation inhibitor for cartilage tissue engineering," *Tissue Eng. Part A*, vol. 15, no. 8, pp. 2309–13, Aug. 2009.

[52] A. Ringle, M. Richardson, F. Juthier, N. Rousse, A. S. Polge, A. Coisne, A. Duva-Pentiah, A. Ben Abda, C. Banfi, D. Montaigne, A. Vincentelli, and A. Prat, "Ross

procedure is a safe treatment option for aortic valve endocarditis: Long-term follow-up of 42 patients," *Int. J. Cardiol.*, vol. 203, pp. 62–8, Jan. 2016.

[53] I. Prasertsung, S. Kanokpanont, T. Bunaprasert, V. Thanakit, and S. Damrongsakkul, "Development of acellular dermis from porcine skin using periodic pressurized technique," *J. Biomed. Mater. Res. B. Appl. Biomater.*, vol. 85, no. 1, pp. 210–9, Apr. 2008.

[54] C. Alberti, "Tissue engineering technologies: just a quick note about transplantation of bioengineered donor trachea and augmentation cystoplasty by de novo engineered bladder tissue," *G. Chir.*, vol. 30, no. 11–12, pp. 514–9, Jan. .

[55] H. C. Ott, T. S. Matthiesen, S.-K. Goh, L. D. Black, S. M. Kren, T. I. Netoff, and D. a Taylor, "Perfusion-decellularized matrix: using nature's platform to engineer a bioartificial heart," *Nat. Med.*, vol. 14, no. 2, pp. 213–221, 2008.

[56] H. Kitahara, H. Yagi, K. Tajima, K. Okamoto, A. Yoshitake, R. Aeba, M. Kudo, I. Kashima, S. Kawaguchi, A. Hirano, M. Kasai, Y. Akamatsu, H. Oka, Y. Kitagawa, and H. Shimizu, "Heterotopic transplantation of a decellularized and recellularized whole porcine heart," *Interact. Cardiovasc. Thorac. Surg.*, p. ivw022, 2016.

[57] M.-T. Kasimir, E. Rieder, G. Seebacher, A. Nigisch, B. Dekan, E. Wolner, G. Weigel, and P. Simon, "Decellularization does not eliminate thrombogenicity and inflammatory stimulation in tissue-engineered porcine heart valves," *J. Heart Valve Dis.*, vol. 15, no. 2, pp. 278–86; discussion 286, Mar. 2006.

[58] F. Boccafoschi, M. Botta, L. Fusaro, F. Copes, M. Ramella, and M. Cannas, "Decellularized biological matrices: an interesting approach for cardiovascular tissue repair and regeneration," *J. Tissue Eng. Regen. Med.*, Oct. 2015.

[59] P. Zou, X. Yang, J. Wang, Y. Li, H. Yu, Y. Zhang, and G. Liu, “Advances in characterisation and biological activities of chitosan and chitosan oligosaccharides,” *Food Chem.*, vol. 190, no. 12, pp. 1174–1181, 2016.

[60] W.-H. Zimmermann, “Biomechanical regulation of in vitro cardiogenesis for tissue-engineered heart repair,” *Stem Cell Res. Ther.*, vol. 4, no. 6, p. 137, 2013.

[61] M. O. Platt and W. A. Shockey, “Endothelial cells and cathepsins: Biochemical and biomechanical regulation,” *Biochimie*, vol. 122, pp. 314–323, 2015.

[62] C. Wang, M. Chen, S. Liu, Y. Liu, J. Jin, and Y. Zhang, “Spatial distribution of wall shear stress in common carotid artery by color Doppler flow imaging,” *J. Digit. Imaging*, vol. 26, no. 3, pp. 466–71, 2013.

[63] L. A. Hidalgo-Bastida, S. Thirunavukkarasu, S. Griffiths, S. H. Cartmell, and S. Naire, “Modeling and design of optimal flow perfusion bioreactors for tissue engineering applications,” *Biotechnol. Bioeng.*, vol. 109, no. 4, pp. 1095–1099, 2012.

[64] N. K. Weidenhamer and R. T. Tranquillo, “Influence of cyclic mechanical stretch and tissue constraints on cellular and collagen alignment in fibroblast-derived cell sheets,” *Tissue Eng. Part C. Methods*, vol. 19, no. 5, pp. 386–95, 2013.

[65] V. Barron, C. Brougham, K. Coghlan, E. McLucas, D. O’Mahoney, C. Stenson-Cox, and P. E. McHugh, “The effect of physiological cyclic stretch on the cell morphology, cell orientation and protein expression of endothelial cells,” *J. Mater. Sci. Mater. Med.*, vol. 18, no. 10, pp. 1973–1981, 2007.

[66] R. Nuccitelli, “Endogenous ionic currents and DC electric fields in multicellular animal tissues,” *Bioelectromagnetics*, vol. Suppl 1, pp. 147–157, 1992.

[67] I. Jacobs, K. Sunde, C. D. Deakin, M. F. Hazinski, R. E. Kerber, R. W. Koster, L. J. Morrison, J. P. Nolan, and M. R. Sayre, “Part 6: Defibrillation: 2010 International Consensus on Cardiopulmonary Resuscitation and Emergency Cardiovascular Care Science with Treatment Recommendations,” *Circulation*, vol. 122, no. 16 SUPPL. 2, 2010.

[68] S. Pietronave, A. Zamperone, F. Oltolina, D. Colangelo, A. Follenzi, E. Novelli, M. Diena, A. Pavesi, F. Consolo, G. B. Fiore, M. Soncini, and M. Prat, “Monophasic and Biphasic Electrical Stimulation Induces a Precardiac Differentiation in Progenitor Cells Isolated from Human Heart,” *Stem Cells Dev.*, vol. 00, no. 00, pp. 1–11, 2014.

[69] D. R. Merrill, M. Bikson, and J. G. R. Jefferys, “Electrical stimulation of excitable tissue: Design of efficacious and safe protocols,” *J. Neurosci. Methods*, vol. 141, no. 2, pp. 171–198, 2005.

[70] M. C. Barsotti, F. Felice, A. Balbarini, and R. Di Stefano, “Fibrin as a scaffold for cardiac tissue engineering,” *Biotechnol. Appl. Biochem.*, vol. 58, no. 5, pp. 301–10.

[71] A. Gandaglia, R. Huerta-Cantillo, M. Comisso, R. Danesin, F. Ghezzo, F. Naso, A. Gastaldello, E. Schittullo, E. Buratto, M. Spina, G. Gerosa, and M. Dettin, “Cardiomyocytes in vitro adhesion is actively influenced by biomimetic synthetic peptides for cardiac tissue engineering,” *Tissue Eng. Part A*, vol. 18, no. 7–8, pp. 725–36, Apr. 2012.

[72] K. L. Fujimoto, K. C. Clause, L. J. Liu, J. P. Tinney, S. Verma, W. R. Wagner, B. B. Keller, and K. Tobita, “Engineered fetal cardiac graft preserves its cardiomyocyte proliferation within postinfarcted myocardium and sustains cardiac

function," *Tissue Eng. Part A*, vol. 17, no. 5–6, pp. 585–96, Mar. 2011.

[73] P. Anversa, J. Kajstura, M. Rota, and A. Leri, "Regenerating new heart with stem cells," *J. Clin. Invest.*, vol. 123, no. 1, pp. 62–70, Jan. 2013.

[74] G. A. Villalona, B. Udelsman, D. R. Duncan, E. McGillicuddy, R. F. Sawh-Martinez, N. Hibino, C. Painter, T. Mirensky, B. Erickson, T. Shinoka, and C. K. Breuer, "Cell-seeding techniques in vascular tissue engineering," *Tissue Eng. Part B. Rev.*, vol. 16, no. 3, pp. 341–50, Jun. 2010.

[75] P. Camelliti, T. K. Borg, and P. Kohl, "Structural and functional characterisation of cardiac fibroblasts," *Cardiovasc. Res.*, vol. 65, no. 1, pp. 40–51, Jan. 2005.

[76] T. Azar, J. Sharp, and D. Lawson, "Heart rates of male and female Sprague-Dawley and spontaneously hypertensive rats housed singly or in groups," *J. Am. Assoc. Lab. Anim. Sci.*, vol. 50, no. 2, pp. 175–84, Mar. 2011.

[77] M. Radisic, H. Park, H. Shing, T. Consi, F. J. Schoen, R. Langer, L. E. Freed, and G. Vunjak-Novakovic, "Functional assembly of engineered myocardium by electrical stimulation of cardiac myocytes cultured on scaffolds," *Proc. Natl. Acad. Sci. U. S. A.*, vol. 101, no. 52, pp. 18129–18134, 2004.

[78] M. N. Hirt, A. Hansen, and T. Eschenhagen, "Cardiac tissue engineering: state of the art," *Circ. Res.*, vol. 114, no. 2, pp. 354–367, 2014.

[79] Y. Zhang, T.-S. Li, S.-T. Lee, K. A. Wawrowsky, K. Cheng, G. Galang, K. Malliaras, M. R. Abraham, C. Wang, and E. Marbán, "Dedifferentiation and Proliferation of Mammalian Cardiomyocytes," *PLoS One*, vol. 5, no. 9, p. e12559, 2010.

[80] M. N. Hirt, J. Boeddinghaus, A. Mitchell, S. Schaaf, C. Börnchen, C. Müller, H.

Schulz, N. Hubner, J. Stenzig, A. Stoehr, C. Neuber, A. Eder, P. K. Luther, A. Hansen, and T. Eschenhagen, “Functional improvement and maturation of rat and human engineered heart tissue by chronic electrical stimulation,” *J. Mol. Cell. Cardiol.*, vol. 74, pp. 151–161, 2014.

[81] J. Xu, W. Wang, C. C. Clark, and C. T. Brighton, “Signal transduction in electrically stimulated articular chondrocytes involves translocation of extracellular calcium through voltage-gated channels,” *Osteoarthr. Cartil.*, vol. 17, no. 3, pp. 397–405, 2009.

[82] J. J. H. Chong, X. Yang, C. W. Don, E. Minami, Y.-W. Liu, J. J. Weyers, W. M. Mahoney, B. Van Biber, S. M. Cook, N. J. Palpant, J. A. Gantz, J. A. Fugate, V. Muskheli, G. M. Gough, K. W. Vogel, C. A. Astley, C. E. Hotchkiss, A. Baldessari, L. Pabon, H. Reinecke, E. A. Gill, V. Nelson, H.-P. Kiem, M. A. Laflamme, and C. E. Murry, “Human embryonic-stem-cell-derived cardiomyocytes regenerate non-human primate hearts,” *Nature*, vol. 510, no. 7504, pp. 273–277, 2014.

[83] S. J. Kattman, A. D. Witty, M. Gagliardi, N. C. Dubois, M. Niapour, A. Hotta, J. Ellis, and G. Keller, “Stage-Specific Optimization of Activin/Nodal and BMP Signaling Promotes Cardiac Differentiation of Mouse and Human Pluripotent Stem Cell Lines,” *Cell Stem Cell*, vol. 8, no. 2, pp. 228–240, 2011.

[84] M. Mercola, P. Ruiz-lozano, and M. D. Schneider, “Cardiac muscle regeneration : lessons from development Cardiac muscle regeneration : lessons from development,” no. 858, pp. 299–309, 2011.

[85] Y. Liu and R. J. Schwartz, “A driver of cardiac cell fate determination © 2013

Landes Bioscience," vol. 4, no. 3, pp. 92–96, 2013.

[86] M. a Laflamme, K. Y. Chen, A. V Naumova, V. Muskheli, J. a Fugate, S. K. Dupras, H. Reinecke, C. Xu, M. Hassanipour, S. Police, C. O'Sullivan, L. Collins, Y. Chen, E. Minami, E. a Gill, S. Ueno, C. Yuan, J. Gold, and C. E. Murry, "Cardiomyocytes derived from human embryonic stem cells in pro-survival factors enhance function of infarcted rat hearts," *Nat. Biotechnol.*, vol. 25, no. 9, pp. 1015–1024, 2007.

[87] J. Krishnan, P. Ahuja, S. Bodenmann, D. Knapik, E. Perriard, W. Krek, and J. C. Perriard, "Essential role of developmentally activated hypoxia-inducible factor la for cardiac morphogenesis and function," *Circ. Res.*, vol. 103, no. 10, pp. 1139–1146, 2008.

[88] R. Bohuslavová, F. Kolář, L. Kuthanová, J. Neckář, A. Tichopád, and G. Pavlinkova, "Gene expression profiling of sex differences in HIF1-dependent adaptive cardiac responses to chronic hypoxia," *J. Appl. Physiol.*, vol. 109, no. 4, pp. 1195–202, 2010.

[89] J.-L. Balligand and P. J. Cannon, "Nitric Oxide Synthases and Cardiac Muscle : Autocrine and Paracrine Influences," *Arterioscler. Thromb. Vasc. Biol.*, vol. 17, no. 10, pp. 1846–1858, Oct. 1997.

[90] J. Shoag and Z. Arany, "Regulation of Hypoxia-Inducible Genes by PGC-1," *Arterioscler. Thromb. Vasc. Biol.*, vol. 30, no. 4, pp. 662–666, 2010.

[91] L. Wang, Y. Cui, M. Tang, X. Hu, H. Luo, J. Hescheler, and J. Xi, "Puerarin facilitates T-tubule development of murine embryonic stem cell-derived cardiomyocytes," *Cell. Physiol. Biochem.*, vol. 34, no. 2, pp. 383–92, 2014.

[92] M. Terashima, N. Inoue, Y. Ohashi, and M. Yokoyama, “Relationship between coronary plaque formation and NAD(P)H oxidase-derived reactive oxygen species - comparison of intravascular ultrasound finding of atherosclerotic lesions with histochemical characteristics,” *Kobe J. Med. Sci.*, vol. 53, no. 3, pp. 107–17, Jan. 2007.

[93] K. L. Kuo, S. C. Hung, Y. P. Lin, C. F. Tang, T. S. Lee, C. P. Lin, and D. C. Tarng, “Intravenous Ferric Chloride Hexahydrate Supplementation Induced Endothelial Dysfunction and Increased Cardiovascular Risk among Hemodialysis Patients,” *PLoS One*, vol. 7, no. 12, 2012.